Utrecht University

Master's thesis

The use of stable isotope analysis to reconstruct paleoenvironments and paleoclimate in the late Pleistocene (MIS 5) of the North Sea Basin

by

Koen Modderman
5974372

14-06-2023

Department of Earth Sciences, Utrecht University, Princetonlaan 8A, 3584 CB, Utrecht, the Netherlands
TNO - Geological Survey of the Netherlands, Princetonlaan 6, 3508 TA, Utrecht, the Netherlands

Supervisors:
Prof. Dr. Lucas Lourens
Dr. Frank Wesselingh

Abstract

Stable isotope analysis is a widely used method for reconstructing the paleoenvironment and -climate. Isotope composition of foraminiferal tests and mollusc shells are adequate proxies as their isotope uptake for shell carbonate formation is representative for the isotopic composition of ambient water. The oxygen and carbon isotope ratios can provide information about (changes in) paleotemperature and paleosalinity. For paleosalinity, a mixing line framework with freshwater and seawater endmembers can provide insights into the temporal variability of paleosalinity. Here we show that reconstructing paleoenvironment and paleoclimate in MIS5 of the North Sea Basin with stable isotopes is taxon dependent. We found that the isotopic composition of mollusc shells largely reflects temperature of ambient waters. Furthermore, we found that the isotopic composition of foraminifera shells of *Ammonia beccarii* is largely influenced by salinity. Reconstruction shows a shift during MIS5e in the Amersfoort Basin from polyhaline to euhaline conditions and back with an increasing impact of the Rhine River, and a three-stage temperature evolution during MIS5a in the southern North Sea. This study is anticipated to be a starting point and recommendation for further reconstruction of paleoenvironment and -climate of MIS5 in the North Sea Basin.

Key words: *stable isotopes, paleoclimate, paleoenvironment, Eemian stage, Early Weichselian stage, foraminifera, molluscs, endmembers, Amersfoort Basin, Brown Bank*

1. Introduction

Understanding past climate fluctuations is important for understanding climate driving mechanisms and giving accurate future climate predictions. The Late Pleistocene witnessed dramatic climate shifts that provide insight into baseline dynamics and responses relevant for today's rapid changes (Helmens, 2014). The Eemian period and Weichselian period together form the Late Pleistocene. The last interglacial (MIS5) encompasses the Eemian optimum (MIS5e) and the basal part of the Weichselian (MIS5d-MIS5a) (Helmens, 2014). The Eemian Stage lasted about approximately from 128-116 kyr BP, although the exact age boundaries are uncertain and a slight difference may exist between optimum climatic conditions and the age boundaries for the Eemian/MIS5e (Kasse et al., 2022). The Eemian was characterized by warmer temperatures (0 to +2.0°C) than the current interglacial, the Holocene (Turney et al., 2020). Eustatic sea level was higher (+6.6 to 11.4 m) and the worlds ice sheets were smaller (Turney et al., 2020; Kasse et al., 2022). The current mean global temperature may be slightly lower than they were at the Eemian optimum, but most recent projections indicate that by 2030 global warming will reach 1.5°C if temperatures remain increasing at the current rates (IPCC, 2021), levelling Eemian temperatures. The Early Weichselian encompasses MIS 5d-a and lasted up to approximately 70 kyr BP (Helmens, 2014). The substage is characterized by temperature fluctuations and contains two colder stadials (MIS5d and MIS5b) and two warmer interstadials (MIS5c and MIS5a: Helmens, 2014). Global temperatures were colder than today, and sea levels could be 60 to 70 m below those of today during stadials (Wohlfarth, 2013). Studies of past climates have the potential to elucidate effects of future climate (Katrantsiotis et al., 2021). The Eemian serves as a reference that provides natural analogue settings for the predicted climate conditions at the end of the 21st century (Brewer et al., 2008; Kantrantsiotis et al., 2021; Kasse et al., 2022). Studying the Eemian climate and ecosystems allows us to understand the climatic evolution throughout an interglacial lacking anthropogenic impact (Brewer et al., 2008).

Recently, two new continuous cores were derived from the Amersfoort Basin that provide a detailed record of the marine sediments of the Eemian. The Eemian interglacial deposits are excellent preserved and are rich in diatoms, foraminifera, and molluscs (Kasse et al., 2022). Borehole B32B2417 is located near the depocenter of the Amersfoort Basin and contains an almost continuous sedimentary record. Also recently, a core was derived from the Brown Bank in the southern North Sea. Borehole SS22-320-VC14 is located close to the Dutch coast and represents MIS5a of the Early Weichselian period. The cores help us to determine environmental successions, aquatic conditions, biodiversity change and climatic conditions for the time interval it represents. This research will focus on the aquatic (paleosalinity) and climatic (paleotemperature) conditions.

Stable isotope analysis is a widely used method for reconstructing aquatic and climatic conditions. The method can be used to reconstruct different physical and chemical parameters (Milano et al., 2020). For example, studying isotopic composition of mollusc shells provides information on past salinity levels (Eisma et al., 1976). There are several processes that can influence the isotopic composition of natural waters (Mook, 1970). For instance, oxygen intake by freshwater molluscs is mainly influenced by temperature and the oxygen isotope value of ambient water (Versteegh, 2010; Milano et al., 2020). Similarly, carbon isotope content of surface water can be influenced by factors such as photosynthesis and isotopic exchange with atmospheric carbon dioxide (Mook, 1970). The isotopic composition of mollusc and foraminiferal shells can carry information about the composition of the ancient ambient water and therefore can tell us a lot about the paleoenvironment and -climate (Mook, 1970; Eisma et al., 1976).

The aim of this thesis is to reconstruct ambient water temperatures and salinity regimes in the Amersfoort MIS5e succession and the Brown Bank MIS5a succession, and to investigate whether molluscs and foraminifera yield similar or additional insights. The isotopic composition of the mollusc and foraminifera shells will be derived from samples of borehole B32B2417 and borehole SS22-320-VC14. The results of isotope analysis will be discussed in relation to the regional paleotemperature and -salinity. To give interpretations, endmembers will be used for the isotopic composition of the sources of the water of the former Amersfoort Basin and the Brown Bank Member. The mollusc and foraminifera faunas are used to constrain environmental settings such as salinity regimes.

2. Geological setting

The Eemian was first described by Harting (1874) and was named after the river Eem, which flows near the city of Amersfoort, The Netherlands (van Leeuwen et al., 2000). The Amersfoort Basin is a glacial basin formed during glaciations of MIS 6 (van Leeuwen et al., 2000). The Eemian stratotype locality in Amersfoort is a key location for studying the Eemian period due to its well-preserved sedimentary record (Cleveringa et al., 2000). Eemian sediments are common in the subsoil of this area because they were deposited in depressions that formed during the Saalian glaciation (Cleveringa et al., 2000; Kasse et al., 2022). This glaciation resulted in the formation of ice-pushed ridges up to 100 m NAP (Dutch Ordnance Datum) and deep glacial basins down to -100 m NAP (Kasse et al., 2022). These basins are filled with lacustrine sediments of the Saalian with Eemian sediments on top with varying thickness (up to 50 m; Cleveringa et al., 2000). The Brown Bank Member is an Early Weichselian clay-rich deposit, spreading across the southern part of the North Sea (Waaijen et al., 2023). The formation is located 85

km off the Dutch coast, 22-16 m below the sea surface, and forms a 25 km long and 2 km wide ridge on the seafloor (Missiaen et al., 2021). It resembles the falling stage of the sea level after the Eemian and has been studied by multiple proxies for past climatic and environmental conditions (Waaijen et al., 2023). The extent of the Eem and the Brown Bank formations and the locations of the studied boreholes are given in figure 1.

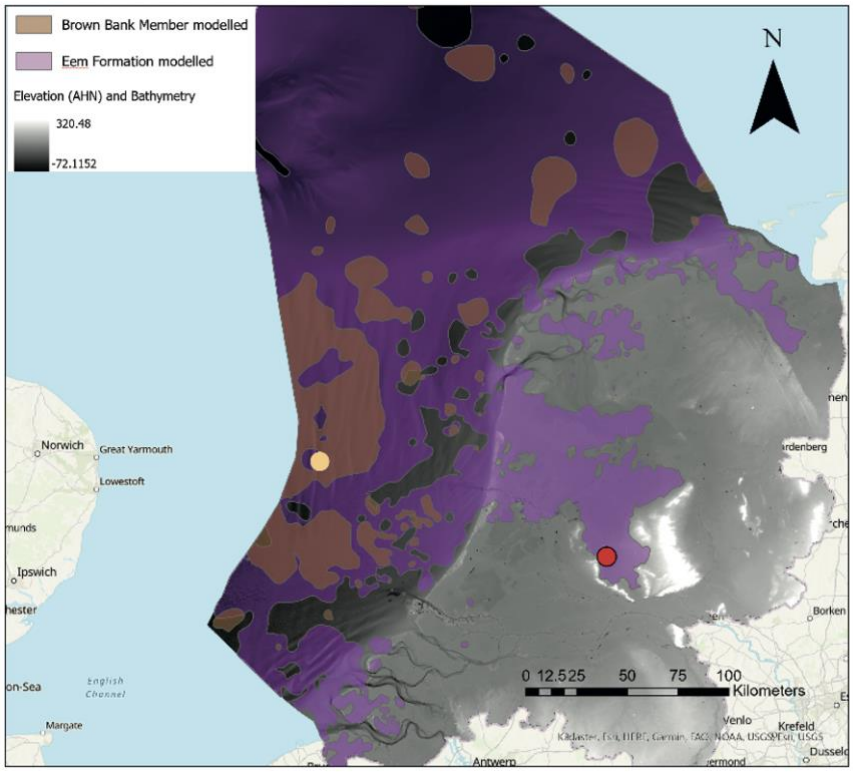

Figure 1: Elevation map of the Netherlands and the southern North Sea, including the Amersfoort (red dot) and Brown Bank (yellow dot) borehole locations and the distribution maps of the Eem (purple) and Brown Bank (brown) formation (obtained via TNO Geological Survey of the Netherlands, 2023).

3. Methods and materials

3.1 Sample preparation

The Eem Formation, an interval of ~26 m (2205-4760 cm below surface) of core B32B2417 (latitude: 52.15451; longitude: 5.41675), was sampled at 5-cm and 10-cm spacing, with exception of 1-cm sampling between 3020-3035 cm. A description of the borehole facies is given in section *3.2.1* and *Appendix 1*. The samples were wet sieved. Fraction >600 μm is used for the selection of the mollusc fauna and fraction 125 μm is used for the selection of the foraminifera. For this study, the samples were picked, cleaned, and used for stable isotope analysis. For measurements of the molluscs, the shells of *Ecrobia ventrosa* were used. For measurements of the foraminifera, the shells of *Ammonia beccarii s.l. (sensu lato)* were used. The Brown Bank Formation, an interval of ~233 cm (0-233 cm below surface) of core SS22-320-VC14 (latitude: 52.70599388; longitude: 3.35766505), was sampled at irregular spacing over a total interval of ~2 m (42-233 cm below surface). A description of the borehole facies is given in section *3.2.2* and *Appendix 2.* The samples from the Brown Bank were prepared at Naturalis Biodiversity Center, Leiden, the Netherlands. For the measurements of the foraminifera, the

shells of *A. beccarii s.l.* were used. For the measurements of the mollusc shells, different species were used.

3.2 Lithology

3.2.1 Lithology at Amersfoort

Late Pleistocene sediments in the central part of the Amersfoort Basin consists of 30-40 m clay intervals, overlain by 25 m layers of marine sands (Cleveringa et al., 2000). The clays are of interest, as it represents the Eemian period. The total Eemian succession of this study is about 25 m thick and is divided into 7 units (table 1). A description of the Amersfoort borehole per section/meter is added as *Appendix 1*. All depths are expressed in cm below surface (cmbs).

Unit L1: 4740-4700 cmbs

The deepest unit completely consists of sand. The top is darker colored and shows some bioturbation. This unit is not of interest for stable isotope analysis as it lacks carbonate fossils. A sandy sequence could indicate local reworking of older outcropping sediments in the ice-pushed ridges near the margin of the glacial basin (Cleveringa et al., 2000). Local reworking of the sediments suggests a dynamic high energy system (Cleveringa et al., 2000).

Unit L2: 4700-4200 cmbs

This unit consists of organically rich clayey sands that contain small shell fragments. It is dark brown color and layered with visible bands. At level 4280-4290 cmbs, a small shell-rich layer is present.

Unit L3: 4200-3205 cmbs

This unit consists of grey to brown clays, which are moderately silty. Throughout the unit, small shell fragments are present. The brown clay shows some layering, whilst the grey clay shows no layering. The transition into clays and presence of *E. ventrosa* and *Peringia ulvae* suggests a transition into a shallow sublittoral and brackish conditions, a low energy environment, probably with the presence of tidal marshes (Cleveringa et al., 2000; de Bruyne, 2020).

Unit L4: 3200-2925 cmbs

At this unit, the clay becomes siltier, consisting of dark grey silty clay, and showing more layering. Shell fragments are still present, not in a notable larger amount than unit *L3*.

Unit L5: 2925-2410 cmbs

This unit consists of very silty clay, having the highest amount of silt of all units present. It also contains the most shell fragments with some paired bivalves present at 2886-2900 cm (of *Polititapes senescens*). It shows brown to grey colors, mostly grey, with visible layering. The presence of *P. senescens* suggests warm conditions (Wesselingh et al., 2023).

Unit L6: 2410-2222 cmbs

This unit consist of dark grey clay that contains plant remains. Layering is still present, while shells disappear upwards. This suggests a change towards a freshwater environment.

Unit L7: 2222-2205 cmbs

This unit consists of dark organically rich crumbly clay, lacking shell fragments but with common organic material and plant remains.

Depth (cmbs)	Lithology	Assumed depositional environment	Unit
4740-4700	Sand	Marginal marine, high energy conditions	L1
4700-4200	Organically rich clayey sands (with a small shell rich layer at level 4280-4290 cmbs)	Marginal marine, high energy conditions	L2
4200-3205	Moderately silty clay with shell fragments	Shallow sublittoral, brackish, intertidal, low energy conditions	L3
3200-2925	Silty clay with shell fragments	Shallow sublittoral, brackish, intertidal, low energy conditions	L4
2925-2410	Very silty clay with shells	Shallow sublittoral, brackish, intertidal, low energy conditions, warm temperatures	L5
2410-2222	Clay with plant remains	Shallow, freshwater conditions	L6
2222-2205	Organic rich clay with plant remains	Shallow, freshwater conditions	L7

Table 1: Lithology units and first interpretation of the Eem Formation deposits at the Amersfoort borehole.

3.2.2 Lithology at the Brown Bank Member

The Brown Bank Member is a clay rich Early Weichselian deposit and has been studied with multiple proxies (Waaijen et al., 2023). The lithology can be divided into 5 units (table 2), based on the lithology overview in *Appendix 2*. The length of the studied core interval of core SS22-320-VC14 is 233 cm. The foraminifera and molluscs used for stable isotope analysis are retrieved at depths between 42-233 cmbs.

Unit L1: 233-193 cmbs

This unit is made up of brown-green silty clay and fine sand laminae with micas throughout the unit. It contains a grey layer at 221-222 cmbs. The clay indicates low energetic, shallow marine conditions (Waaijen et al., 2023).

Unit L2: 193-119 cmbs

This unit is made up of black-grey medium sand which is fining upwards into fine grey sand. It contains shell fragments and medium sized pebbles throughout the unit. The sand suggests open marine conditions (Waaijen et al., 2023).

Unit L3: 119-52 cmbs

This unit is fining upwards from fine sand to clayey silt, which is grey to dark grey. It contains shell fragments and small pebbles throughout the unit. The transition to smaller grain sizes may suggest an increase in deltaic influence, where the delta came closer to the site (Waaijen et al., 2023).

Unit L4: 52-25 cmbs

This unit consists of dark grey bioturbated stiff clay. At has an organic rich lens at 32-33 cmbs and a lens of fine sand at 51-54 cmbs. The clay suggests a transition back to low energetic, shallow marine conditions (Waaijen et al., 2023)

Unit L5: 25-0 cmbs
This unit is made up of brownish grey very fine sand and clay. It contains shell fragments throughout and has 1 elongated rounded pebble at a depth of 23 cmbs and 3 rounded pebbles at 18-20 cmbs.

Depth (cmbs)	Lithology	Assumed depositional environment	Unit
233-193	Silty clay with fine sand laminae	Shallow marine conditions, low energy	L1
193-119	Medium-coarse sand fining upwards with shell fragments	Open marine conditions, high energy	L2
119-52	Clayey silt with bodies of fine sand	Marine conditions, deltaic influence	L3
52-25	Stiff clay with bioturbation (with an organic rich lens at 32cm)	Shallow marine conditions, low energy	L4
25-0	Very fine sand and clay with shell fragments	Shallow marine conditions, low energy	L5

Table 2: Lithology units and first interpretation of the Early Weichselian deposits at the Brown Bank borehole (pers.com. Ruth Pels).

3.3 Stable isotope analysis

Oxygen ($\delta^{18}O$) and carbon isotope ($\delta^{13}C$) analysis were performed on benthic foraminifera (*A. beccarii s.l.*) and molluscs (*E. ventrosa* for the Amersfoort borehole samples and a number of different species for the Brown Bank samples (see section 3.5)) to reconstruct temperature and salinity properties of the ancient water bodies. The foraminifera were picked from size fraction 125 μm and the molluscs which were picked from size fraction >600 μm. After picking, the samples were crushed and cleaned in an ultrasonic bath for 20-30 seconds. After drying overnight in a 45°C oven, they were measured using a Thermo GasBench-II coupled to a Thermo Delta-V Advantage. All samples were calibrated using the in-house standard "Naxos" and the TS-Limestone "NBS-19" that are used as international standards. All values are expressed in the standard delta notation relative to the Vienna Pee Dee Belemnite (VPDB). Some samples were run more than once if the sample material was sufficiently abundant. The weighed amount for each run per sample varied between 25-100 μm, dependent on the abundancy of the sample material. $\delta^{18}O$ values are usually expressed in VPDB, but also can be calculated relative to the Vienna Standard Mean Ocean Water (VSMOW) (Versteegh et al., 2010). The $\delta^{13}C$ isotope content will represent the dissolved inorganic carbon (DIC), that consists mainly of bicarbonate (HCO_3^-) and low concentrations of H_2CO_3 and CO_3^{2-} (Versteegh et al., 2010).

3.4 Foraminifera

Foraminifera were present at most locations throughout the Amersfoort core. All foraminifera were separated from the samples with wet sieving at size fraction 125 μm and picking. For further studies for the Amersfoort core, different foraminiferal specimens were picked. For this study, only *A. beccarii* (fig. 2) was used for stable isotope analysis. This species is abundant throughout the core. The size of

the foraminifera used for stable isotope analysis varied between ~200-600 μm and for every measurement a total amount of 5-25 foraminifera were used. For the stable isotope analysis of the samples retrieved from the Brown Bank core, also only *A. beccarii* was used which facilitated direct comparison between the two cores. The Brown Bank specimens were on average larger than those from the Amersfoort samples, so for every measurement only 5 specimens were used.

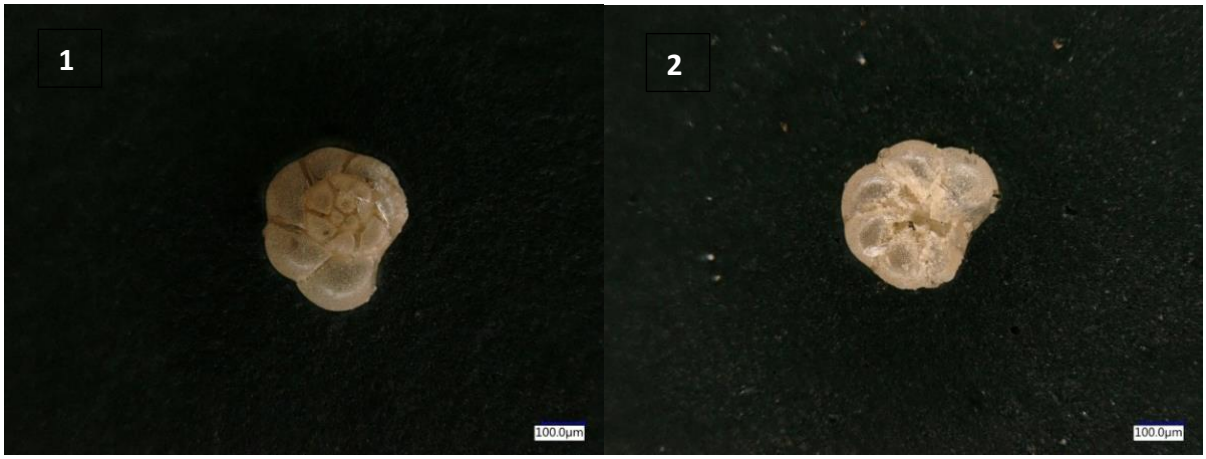

Figure 2: Ammonia beccarii s.l. spiral side (1) and A. beccarii s.l. umbilical side (2).

The foraminiferal genus *Ammonia* is one of the two most common genera of foraminifera in estuaries and shallow marine environments (Hayward et al., 2019; Hayward et al., 2021). For three decades, all *Ammonia* species were identified as *A. beccarii* (fig. 2), but studies showed that this was not the case and that the number of *Ammonia* species living worldwide is likely to exceed 25-30 (Hayward et al., 2019).

3.5 Molluscs

Due to yield problems, mollusc fossils only had a partial coverage at the Amersfoort core, at a depth between 2530-3475 cm. The complete borehole has predominantly been investigated for foraminifera, but the restricted intervals where both foraminifera and molluscs were present will be compared. Two mollusc species were dominantly present: *Ecrobia ventrosa* and *Peringia ulvae*. The two species look very alike but can be distinguished by their size and shape. *Ecrobia ventrosa* has a more convex whorl profile (fig. 2). Shells were crushed because they were too large for preparation for the measurement. Five specimens of *E. ventrosa* per sample were used for analyses.

In the Netherlands, *E. ventrosa* can be found in shallow brackish water in coastal areas, but also on salt marshes in pools with a freshwater supply (de Bruyne, 2020). They prefer to live in shallow brackish waters in coastal areas, with salinities between 4-25‰ (de Bruyne, 2020). They can be found in masses on the bottom, between plants and colonies of bryozoans (de Bruyne, 2020). Some of the *E. ventrosa* specimens in the Amersfoort borehole were overgrown by bryozoans (fig. 2-5 and 2-6), which are colony-forming sessile invertebrates (Law, 2013). The fine preservation of these bryozoans clearly indicates very low energy condition in the depositional environment.

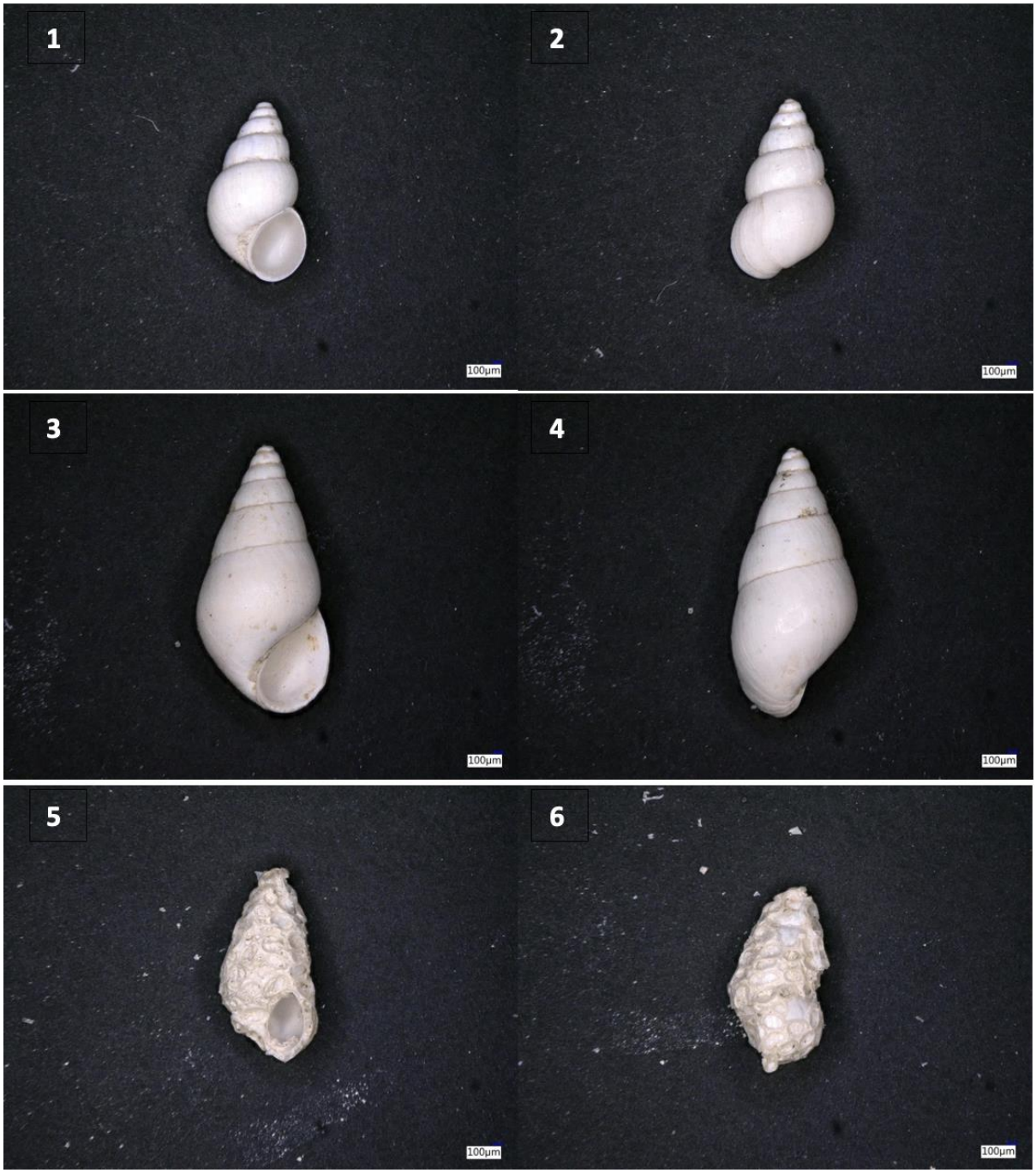

Figure 3: Ecrobia ventrosa front (1) and back (2), Peringia ulvae front (3) and back (4), and E. ventrosa with bryozoans front (5) and back (6).

For the stable isotope analysis of the Brown Bank samples, different mollusc species are used. Some of these species may be *in situ*, whilst other samples may be reworked and originate from a different climate and environment. Criteria used to assess a likely in-situ occurrence are the presence of very fine surface details, presence of periostracum, presence of paired valves. After separation of potential in situ specimens, the fauna must consist of ecological consistent species (pers.com. Frank Wesselingh). In total eight species were used for stable isotope analysis, seven of which are considered to represent an *in situ* fauna (table 3).

Depth (cmbs)	Species	Associated climatic conditions
042-70	*Aequipecten opercularis@*	Warm-temperate
042-70	*Ennucula tenuis*	Arctic
070-100	*Ennucula tenuis*	Arctic
100-117	*Macoma calcaraea*	Arctic
117-135	*Macoma calcaraea*	Arctic
117-135	*Macoma baltica*	Temperate
135-161	*Abra prismatica*	Temperate
135-161	*Abra prismatica*	Temperate
161-187	*Spisula elliptica*	Temperate
161-187	*Astarte montagui*	Arctic
161-187	*Abra prismatica*	Temperate
187-193	*Astarte montagui*	Arctic
187-193	*Nucula nucleus*	Temperate
187-193	*Spisula elliptica*	Temperate

Table 3: Mollusc species, found in the Brown Bank core, with their associated depth and climatic conditions (pers.com. Frank Wesselingh). @The Aequipecten opercularis is considered to be a reworked specimen: it has a worn brown-orange appearance, whereas the in situ component of the sample consists of partially paired bivalves with periostracum and fine surface details.

3.6 Endmembers

3.6.1 Endmembers and changes in isotopic composition

The concept of endmembers is important for understanding and quantifying isotopic mixing in natural systems. It provides a framework, where the isotopic composition of mixed waters is an intermediate between the compositions of an endmember (Kendall & Caldwell, 1998). In terms of isotopic mixing, an "endmember" refers to a pure or nearly pure sample of a particular isotopic composition that is assumed to represent one of the sources contributing to the mixture. Measured values of the shell $\delta^{18}O$ and $\delta^{13}C$ are a result of ambient water $\delta^{18}O$ and $\delta^{13}C$ values (Eisma et al., 1976; Versteegh et al., 2010), providing information about the isotopic composition of the body of water. For example, within an estuary, stable isotope ratios will reflect mixing of ratios of a river and the marine endmembers (Mook, 1970). In general, $\delta^{18}O$ values of the surface water in an estuary is influenced by the mixing of river water and seawater, but other factors such as evaporation and precipitation can modify isotope ratios (Mook, 1970). Similarly, the $\delta^{13}C$ value of the surface water in an estuary can also be influenced by mixing of different water sources, as well as other factors such as photosynthesis and isotopic exchange with atmospheric carbon dioxide (Mook, 1970).

Mook (1970) discussed these processes and distinguished three main categories:

1. Isotopic fractionation during evaporation and condensation processes can cause variations in the $\delta^{18}O$ values of precipitation and surface water. As water evaporates, the lighter isotopes (e.g., ^{16}O) tend to vaporize more easily than the heavier isotopes (e.g., ^{18}O), leading to an increase in the $\delta^{18}O$ ratio of the remaining water. Similarly, during condensation, the heavier isotopes tend to

condense more readily, leading to a decrease in the $\delta^{18}O$ value of the remaining water (NASA Earth Observatory, 2005).

2. Biological processes, such as photosynthesis and respiration, can cause variations in the $\delta^{13}C$ values of natural waters. Phytoplankton tends to preferentially incorporate the lighter isotope of carbon (^{12}C) into organic matter during photosynthesis, leading to an increase in the $\delta^{13}C_{DIC}$ value of the surface water (Ge et al., 2022).
3. Geochemical processes, such as weathering and dissolution, can also affect the $\delta^{13}C$ and $\delta^{18}O$ values of natural waters. For example, as water flows through rocks and sediments, it can dissolve minerals that are enriched in certain isotopes. This can lead to variations in the isotopic composition of the water.

Furthermore, the isotopic values of a river endmember like the Rhine display seasonal cycle because of seasonal variation in the amount and composition of the water (Versteegh et al., 2010). For instance, $\delta^{18}O$ values are higher in summer due to evaporation and enriched summer precipitation and $\delta^{13}C_{DIC}$ values are rising in early summer due to removal of ^{12}C from the DIC pool by phytoplankton photosynthesis (Versteegh et al., 2010). This seasonal variation gives a range instead of an exact value. For comparing the results of this study, average ratios will be used.

The isotopic composition is also dependent on salinity. If salinity would be the sole driver of isotopic composition the relation between salinity and the isotopic composition of the carbonate can be represented by:

$$\delta^{18}O_{VMOW} = (1 - \rho)\delta^{18}O_{VSMOW}(fresh) + \rho\delta^{18}O_{VSMOW}(sea)$$

where ρ (= Cl'/Cl'_{marine}) is the degree of brackishness (Eisma et al., 1976). This is a linear relationship between salinity and $\delta^{18}O$ content: 1‰ increase $\delta^{18}O$ equals an increase in salinity of about 3.9‰ (Eisma et al., 1976). A study that investigates the current oxygen isotope composition of water masses within the North Sea is a study by Harwood et al. (2008), which uses a linear mixing line:

$$\delta^{18}O_{VSMOW} = -9.3 + 0.274(S)$$

where S is the salinity. The number -9.3 represents the freshwater endmember value in $‰_{VSMOW}$, but the dominant source of freshwater for this mixing line is the Baltic Sea (Harwood et al., 2008). This relation shows that an increase of 1‰ in $\delta^{18}O$ equals an increase of about 3.7‰ in salinity. A study by Wanamaker et al. (2007) shows the relationship between $\delta^{13}C_{DIC}$ and salinity:

$$\delta^{13}C_{DIC,\ VPDB} = -19.5 + 0.62(S)$$

Where S is salinity in ‰. According to this relation, an increase of 1‰ in $\delta^{13}C_{DIC}$ equals an increase in salinity of approximately 1.6‰. Based on the salinity levels, the salinity of the body of water in question can be classified. The classifications used for this study are based on Por (1972) and are polyhaline (18-30‰), euhaline (30-35‰), and metahaline (35-45‰). Brackish conditions apply within a range of 5-30‰ (Por, 1972). Euryhaline conditions comprises multiple salinity classifications,

whereas euryhaline organisms can survive within a wide range of salinities (Schultz & McCormick, 2012).

Temperature also has influence on the isotopic composition (Eisma et al., 1976). Isotopic values of shell carbonates (expressed in ‰VPDB) are dependent of isotopic values of ambient water (expressed in ‰VSMOW) and the temperature (i.e. Epstein et al, 1953; Bemis et al., 1998):

$$T\ (°C) = 16.5 - 4.81(\delta^{18}O_{shells} - \delta^{18}O_{water})$$

where the $\delta^{18}O_{water}$ is corrected for the VSMOW to VPDB scale by subtracting 0.27‰ (Bemis et al., 1998). This is due to the fractionation between the calcite and the water (Bemis et al., 1998).

If salinity decreases, the $\delta^{18}O$ and $\delta^{13}C$ content decreases, and the isotopic component of the water shifts towards the freshwater component (Eisma et al., 1976). If the temperature decreases, the $\delta^{18}O$ content increases. A study by O'Neil et al. (1969) gives a linear relationship between $\delta^{18}O$ content and temperature for inorganic precipitation of calcite: -0.21‰/°C at 20-30°C (Shimamura et al., 2005), which equals almost 5°C per 1‰ change in $\delta^{18}O$ content. For glacial oceans, Adkins et al. (2002) provides a linear relationship for benthic $\delta^{18}O$ change and temperature of 0.26‰/°C, which equals about 4°C per 1‰ change in $\delta^{18}O$ content.

3.6.2 Defining endmembers

For both the Amersfoort MIS5e and Brown Bank MIS5a succession a riverine and marine endmember was constructed from literature sources. Both are coastal areas where river water is mixing with seawater. One river contributing would be the Rhine (van Leeuwen et al., 2000). In the case of the Brown Bank data, the glacial Rhine will be used as endmember. Glacial river water has a lower $\delta^{18}O$ than interglacial river water, because during glacial periods, much of Earth's water is locked up in the ice that contains a higher ratio of the lighter oxygen isotope ^{16}O (Dansgaard et al., 1993).

Oxygen isotope endmember values

Harwood et al. (2008) provides a current $\delta^{18}O$ value for the river Rhine: -9.8‰$_{VSMOW}$. Versteegh et al. (2009) also provides $\delta^{18}O$ values for shells from the Rhine, that have an average value of -9.1‰$_{VPDB}$ and an average value for Rhine water of -9.2‰$_{VSMOW}$. The average of all obtained endmembers of interglacial river Rhine water will be used for this study, which is -9.5‰$_{VSMOW}$. The $\delta^{18}O$ endmember value for seawater is assumed to be 0.0‰$_{VSMOW}$. The $\delta^{18}O$ values for the shell calcite are expressed in VPDB, while values for water are expressed in VSMOW. For converting the values in VSMOW to VPDB, the relation by Epstein et al. (1953) is used (section *3.6.1*).

Endmembers for the Brown Bank Member are more difficult to obtain. As there is no data of the isotopic composition of the glacial Rhine, we use the isotopic composition of glacier meltwater runoff for the riverine endmember. One study that provides the average $\delta^{18}O$ value for meltwater runoff is from Gurney & Lawrence (2004), that investigates the stable isotopic composition of snow meltwater runoff in a subarctic catchment in Okstindan, Norway. They measured an average value of -13.26‰$_{VSMOW}$. A more recent study is by Chen et al. (2019), that measured the isotopic composition of snow/glacier meltwater runoff in the Tianshan Mountains in Central Asia. They measured an average

value of -12.30‰$_{VSMOW}$ for snow meltwater runoff and -10.46‰$_{VSMOW}$ for glacier meltwater runoff. The average of these endmembers will be used as a reference for the glacial river Rhine, which is -12.01‰$_{VSMOW}$. The glacial seawater endmember differs from the interglacial endmember value. Fractionation of the seawater and growth of the continental ice sheets enriches the $\delta^{18}O$ content of seawater (Schrag et al., 2002). Study shows that the average value for interglacial-glacial global change in $\delta^{18}O$ content for seawater is 1.0 ± 0.1‰$_{VSMOW}$ (Schrag et al., 2002). Furthermore, a study by Beets et al. (2005) shows the values for *A. beccarii s.l.* in the North Sea during MIS8, a glacial period. The values vary between -0.12 and 0.72‰$_{VPDB}$, with an average of 0.30‰. For the glacial seawater endmember, a value of 0.30‰$_{VSMOW}$ will be used.

Carbon isotope endmember values

River water generally has a lower $\delta^{13}C$ value than seawater due to the input of organic matter and inorganic materials that are enriched in the lighter isotope ^{12}C (Mook, 1970; Versteegh, 2010). However, in this study we will be looking at the inorganic fraction ($\delta^{13}C_{DIC}$), which will exclude organic $\delta^{13}C$. The isotopic composition may than be determined by additional sources such as groundwater, isotopic exchange with atmospheric CO_2, chemical weathering of carbonate rocks, photosynthetic activity, and decomposition of organic matter (Mook, 1970; Versteegh, 2010; Yan et al., 2020). The mean value of $\delta^{13}C$ for the oceanic bicarbonate in interglacial North Sea water is about +1.0‰$_{VPDB}$ (Eisma et al., 1976). According to Mook (1970), the $\delta^{13}C$ content of the dissolved bicarbonate in the river Rhine varies between approximately -11 and -9‰. Part of this variation could be affected by exchange in the river itself due to fractionation in combination with a long residence time, and fresh autumn input by precipitation and groundwater (Mook, 1970). The groundwater has a $\delta^{13}C$ value of ~-12‰, which will be taken as an absolute extreme, or endmember, for freshwater $\delta^{13}C_{DIC}$ content.

For the Brown Bank member – as it is formed during the Early Weichselian – the riverine endmember will be based on $\delta^{13}C$ values of arctic rivers. One study that provides $\delta^{13}C_{DIC}$ values for an arctic river is by Gareis & Lesack (2020), that looks at carbon fluxes in river Mackenzie, northwestern Canada. Their results show a narrow range for the $\delta^{13}C_{DIC}$ values: between -6.14 and -6.52‰. For this study, the average will be used as an endmember value. This value is -6.33‰. Similar to the $\delta^{18}O$ value of seawater during glacial periods, the $\delta^{13}C$ value also differs from seawater values during interglacial periods. For example, low isotopic signature of terrestrial carbon was transferred to the glacial ocean during the Last Glacial Maximum (Gebbie et al., 2015). A study by Gebbie et al. (2015) estimated a mean global marine glacial-interglacial change in $\delta^{13}C_{DIC}$ of 0.32 ± 0.1‰, indicating lower values for glacial periods on average. Beets et al. (2005) studies the $\delta^{13}C_{DIC}$ content of the North Sea during MIS8. The values vary between 0.33 and -0.85‰, with an average of -0.26‰. This value will be used as a glacial seawater endmember.

Endmember	$\delta^{18}O$ (‰VSMOW)	$\delta^{18}O$ (‰VPDB)	$\delta^{13}C_{DIC}$ (‰VPDB)
Interglacial seawater (North Sea)	0.00	-0.27	1.00
Glacial seawater (North Sea)	0.30	0.03	-0.26
Interglacial river water (Rhine)	-9.50	-9.77	-12.00
Glacial river water (Rhine)	-12.01	-12.28	-6.33

Table 4: Proposed isotope ratios of the endmembers.

3.6.3 Mixing lines

Mixing lines present a framework in which the position of the samples can be interpreted in terms of contribution of each endmember. Two mixing lines, obtained from Eisma et al. (1976), are also presented and represent the Eemian Rhine and the Wadden Sea. Mixing lines used for the Amersfoort data are the (interglacial) Rhine, Eemian Rhine, and Wadden Sea lines. Mixing lines used for the Brown Bank data are the glacial Rhine and Wadden Sea lines.

Figures 6, 9, and 10 show the relation between $\delta^{18}O$ and $\delta^{13}C$ of foraminifera carbonates and mollusc carbonates of the Amersfoort Basin and the Brown Bank Member and the mixing lines. The higher the $\delta^{18}O$ and $\delta^{13}C$ values become, the larger the influence of the river Rhine was on the isotopic composition of the body of water. The distinguished phases of the data are also shown on the figures. The position and spreading of these phases within the mixing line framework imply certain shifts in environmental conditions in the Eemian period (for Amersfoort) and the Early Weichselian (for the Brown Bank Member).

The obtained mixing lines are linear and can be expressed in their own formula. The different formulas show the relationships between $\delta^{18}O$ and $\delta^{13}C$ and they are as followed:

Rhine: $\delta^{13}C_{VPDB} = 1.37\delta^{18}O_{VPDB} + 1.37$

Glacial Rhine: $\delta^{13}C_{VPDB} = 0.49\delta^{18}O_{VPDB} - 0.27$

Eemian Rhine: $\delta^{13}C_{VPDB} = 1.44\delta^{18}O_{VPDB} + 0.89$

Wadden Sea: $\delta^{13}C_{VPDB} = 0.97\delta^{18}O_{VPDB} + 0.79$

where $\delta^{13}C$ and $\delta^{18}O$ are expressed in ‰ VPDB.

4. Results

4.1.1 Amersfoort succession

The foraminifera isotope ratios for borehole Amersfoort (fig. 4) show shifts and five phases are defined (fig. 5) with their own characteristic ratios (table 5). Phase 1 shows an increasing trend, ending with a negative peak in both carbon and oxygen ratios. Phase 2 shows the highest values for $\delta^{18}O$ and increasing trends, ending with a large decrease in both data. Phase 3 shows a decreasing trend, ending with a large fluctuation of two large peaks in both data. Phase 4 also shows a lot of variation and has a very gradually decreasing trend. Phase 5 shows an increasing trend for the $\delta^{18}O$ data and a decreasing trend for the $\delta^{13}C$ data. Between phase 4 and 5 the data show some remarkable outliers (fig. 5), which are negative for $\delta^{18}O$ and positive for $\delta^{13}C$.

The mollusc and foraminifera data in the studied intervals are not congruent: the mollusc data show lower variability and lower ratios for the $\delta^{18}O$ data. The mollusc data only covers a small part of the borehole, between a depth of 3475-2530cm. The mollusc $\delta^{18}O$ and $\delta^{13}C$ data show covariance but will not be divided into phases. In contrary to the foraminifera data, the mollusc data show $\delta^{13}C$ values that

are higher than the $\delta^{18}O$ values. The $\delta^{13}C$ data as well as the $\delta^{18}O$ data show an increasing trend at 3475-2850 cmbs and a decreasing trend afterwards. The data show a peak at a depth of 2850 cm.

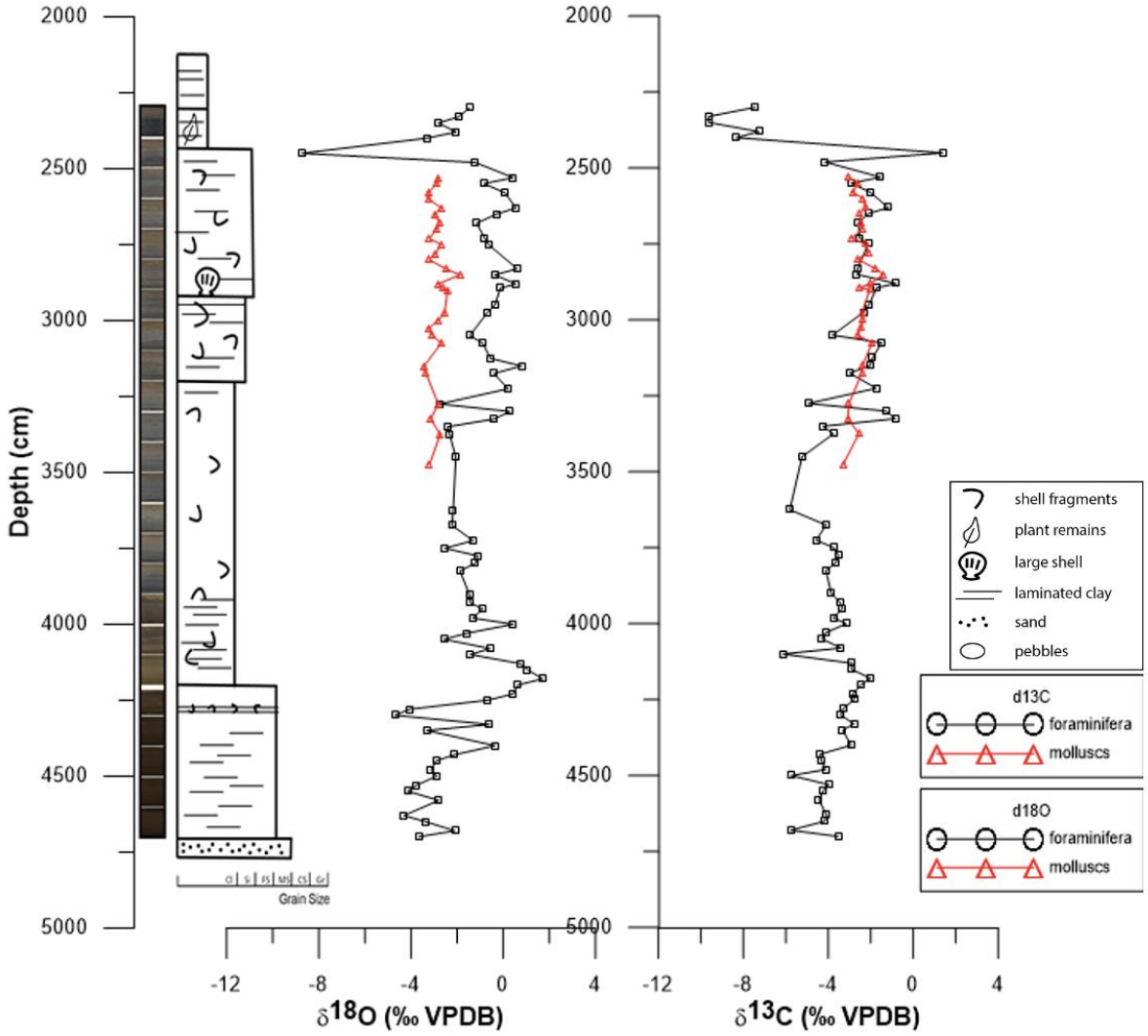

Figure 4: Isotopic values of foraminifera and mollusc shells at the Amersfoort Basin with their corresponding lithology and depth.

Phase	Depth (cmbs)	Range $\delta^{18}O$ (‰VPDB)	Range $\delta^{13}C$ (‰VPDB)	Average $\delta^{18}O$ (‰VPDB)	Average $\delta^{13}C$ (‰VPDB)	Lithology unit
1	4700-4300	-4.31 – -0.35	-5.77 – -2.79	-2.82	-4.13	L2
2	4250-4100	-0.67 – 1.71	-2.90 – -2.01	0.65	-2.64	L2; L3
3	4080-3325	-2.58 – 0.44	-3.15 – -5.81	-1.59	-4.01	L3
4	3225-2450	-1.45 – 0.79	-4.16 – -0.80	-0.31	-2.25	L3; L4; L5
5	2400-2280	-3.32 – -1.46	-9.63 – -7.26	-2.31	-8.46	L5; L6

Table 5: Distinguished phases of the foraminifera data at Amersfoort with their isotopic characteristics and their correlating lithology unit.

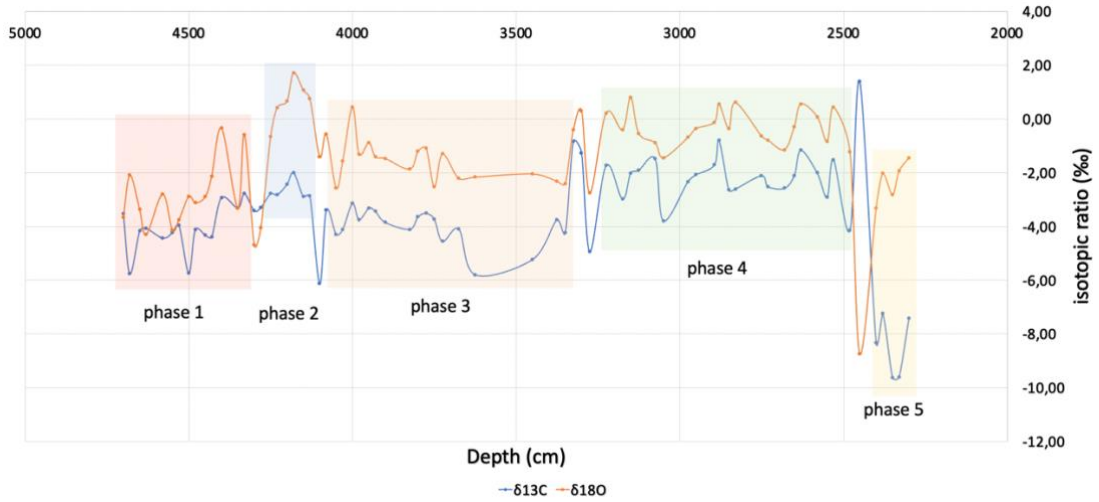

Figure 5: isotopic data and its distinguished phases of foraminifera shells from the Eemian period at the Amersfoort basin.

4.1.2 Positioning in the mixing line framework at Amersfoort

The phase succession shows shifting isotope signatures related to increasing and decreasing salinities and increased influence of the Rhine River. Phase 1 is positioned closely to the mixing lines, while the other phases are drifting outwards (fig. 6). Phase 2 shows a large positive isotopic shift, whereas phase 3 shows a negative shift after. Phase 4 shows the highest isotopic values and a shift towards the marine endmembers. Phase 5 shows the largest shift towards the freshwater endmember, but still deviates largely from the mixing line values.

The mollusc data show consistent lower $\delta^{18}O$ ratios and higher $\delta^{13}C$ ratios and are less spread out; covariance with the foraminifera data is very low. The positioning within the mixing line framework shows a high covariance with the Wadden Sea and the Rhine (fig. 6). The mollusc data deviates far less from the mixing line framework than the foraminifera data.

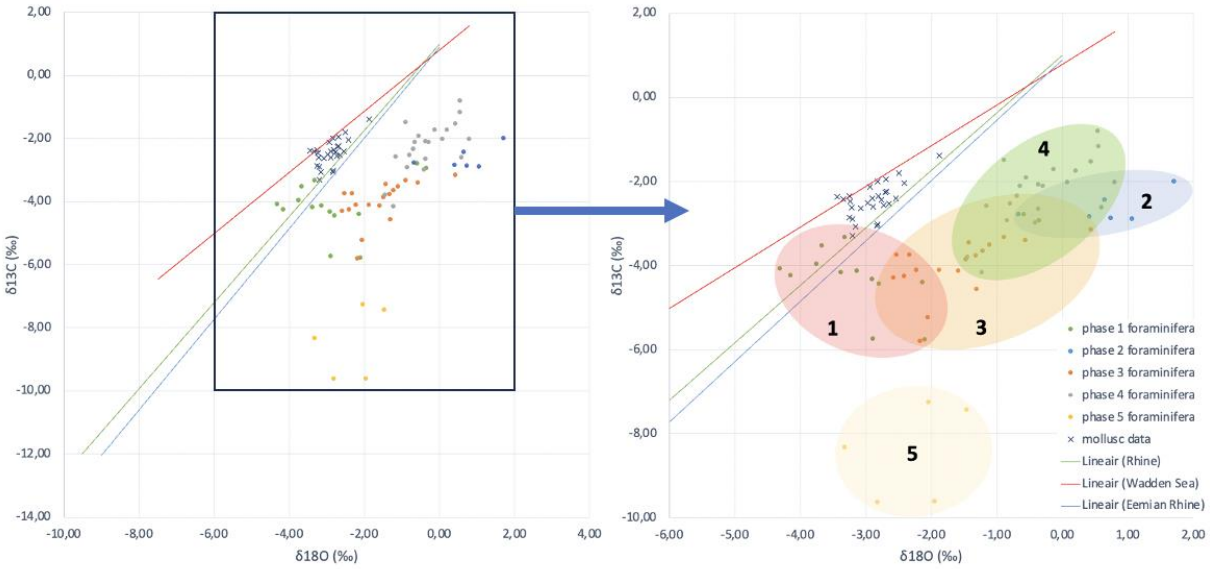

Figure 6: Relation between $\delta^{13}C$ and $\delta^{18}O$ of foraminifera and mollusc shell carbonates in the Amersfoort Basin and the position of the distinguished phases in the mixing line framework.

4.2.1 Brown Bank Succession

The stable isotope ratios for molluscs and foraminifera in the Brown Bank Member are provided in figure 7. One thing that can be noticed when compared to the data of the Amersfoort succession is that, in contrast to the Amersfoort data, the mollusc data show larger values for both oxygen and carbon isotopes than the foraminifera data. Within the data, 3 phases are defined (fig. 8), with their own characteristic ratios (table 6). The first two phases of the datasets show covariance. The end of phase 2, however, shows an increase in $\delta^{18}O$ and a decrease in $\delta^{13}C$. The first phase shows an increasing trend. After the first phase, the data shows a leap towards the second phase, which shows the highest values of $\delta^{18}O$. The second phase shows a decreasing trend after those high values. After the second phase, the third phase shows an increasing trend again.

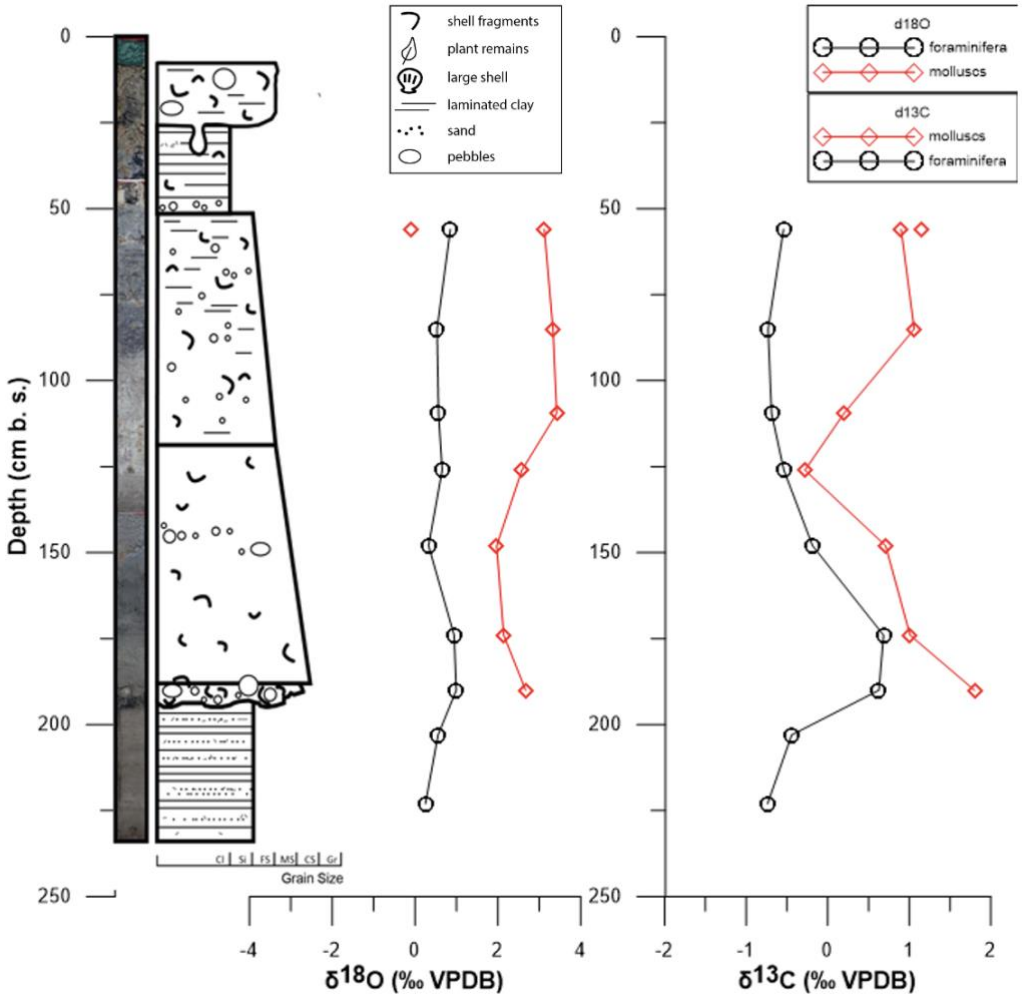

Figure 7: Isotopic values of foraminifera and mollusc shells at the Brown Bank member with their corresponding lithology and depth. The reworked mollusc sample is shown as a separate component at a depth of ~56 cm, while the average value is taken for mollusc samples at other depths.

The mollusc data show larger variations throughout the core depths than the foraminifera data. The lower interval did not yield molluscs (below 2 mbs: fig. 7). Furthermore, one outlier in the data (phase 3; fig. 8) is excluded in the discussion. The $\delta^{18}O$ and $\delta^{13}C$ data show resemblance with the foraminifera data. Distinction of phases is not straightforward, but for foraminifera three phases are described: the upper two match with two phases for the mollusc isotope data (fig. 8). The first phase of the mollusc

data correlates with the phase 2 of the foraminifera data and the second phase of the mollusc data correlates with the phase 3 of the foraminifera data, which is why the mollusc data phases are subdivided into phase 2 and 3. Phase 2 shows a decreasing trend for the $\delta^{13}C$ data as well as the $\delta^{18}O$. Phase 3 has the highest difference in $\delta^{18}O$ and $\delta^{13}C$ ratios and shows an increasing trend for $\delta^{13}C$ but a decreasing trend for $\delta^{18}O$.

Phase	Depth (cm)	Data	Range $\delta^{18}O$ (‰VPDB)	Range $\delta^{13}C$ (‰VPDB)	Average $\delta^{18}O$ (‰VPDB)	Average $\delta^{13}C$ (‰VPDB)	Lithology unit
1	233-193	For	0.25 – 0.55	-0.74 – -0.44	0.40	-0.59	L1
2	193-117	For	0.32 – 0.99	-0.54 – 0.68	0.73	0.15	L2
		Mol	1.66 – 3.30	-0.83 – 2.03	2.35	0.93	
3	117-42	For	0.53 – 0.85	-0.73 – 0.54	0.65	-0.65	L3; L4 (10 cm)
		Mol	3.12 – 3.42	0.20 – 1.51	3.29	0.72	

Table 6: Distinguished phases of the foraminifera (for) and mollusc (mol) data at the Brown Bank Member with their isotopic characteristics and correlating lithology unit.

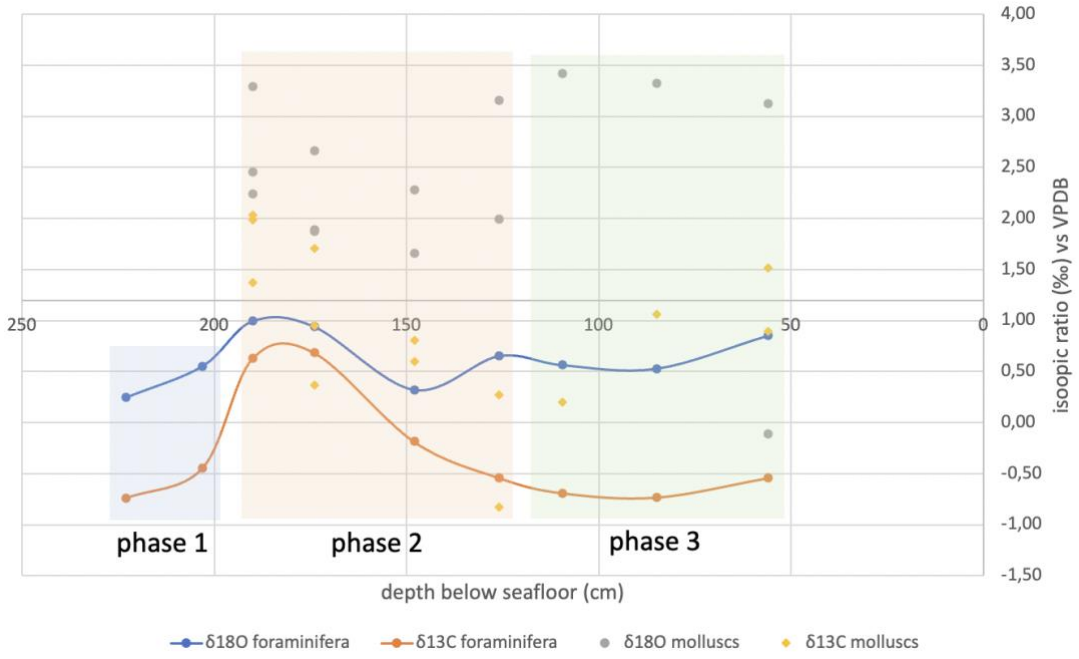

Figure 8: isotopic data and its distinguished phases of foraminifera and mollusc shells from the Early Weichselian succession at the Brown Bank Member. A molluscan outlier is present around a depth of 56 cm at a value of -0,11‰ $\delta^{18}O$ and at 1.51‰ $\delta^{13}C$. This sample is not included in calculations, because it is presumably a reworked component, whilst the other samples are presumably in situ components.

4.2.2 Positioning in the mixing line framework at the Brown Bank Member

The endmember approach to which salinity ranges (restrained by ecological constraints of species) are reasonable low show that the temperature ranges interpreted by the molluscan fauna are much higher than those of the foraminifera. Both datasets show positions outside the mixing line framework with a high concentration in highly marine conditions, suggesting high levels of salinity (fig. 9-10). Not many

samples are used for stable isotope analysis of the Brown Bank, giving little information relative to the Amersfoort succession. Still, shifts can be observed. Phase 2 of the foraminifera (fig. 9) shows various levels of increase in isotopic composition and phase 3 shows an overall decrease towards approximately the same $\delta^{13}C$ values, but higher $\delta^{18}O$ values as phase 1.

The molluscan assemblage shows much wider ranges and consists out of 8 different species, each with their own ecological characteristics and constraints (fig. 11). Phase 1 is more spread out and has the highest $\delta^{13}C$ values (fig. 10). Phase 2 shows an overall increase in $\delta^{18}O$ content. Not all samples shown in figure 11 are shown in figure 10, as one sample is assumed to be a reworked component (the warm-temperature specimen). One thing that can be noticed from this figure, is that the position of the temperature-related species is within high $\delta^{18}O$ values for the cold-temperature-related species, and low $\delta^{18}O$ values for the warm-temperature-related species. The moderate-temperature-related species show average values for $\delta^{18}O$.

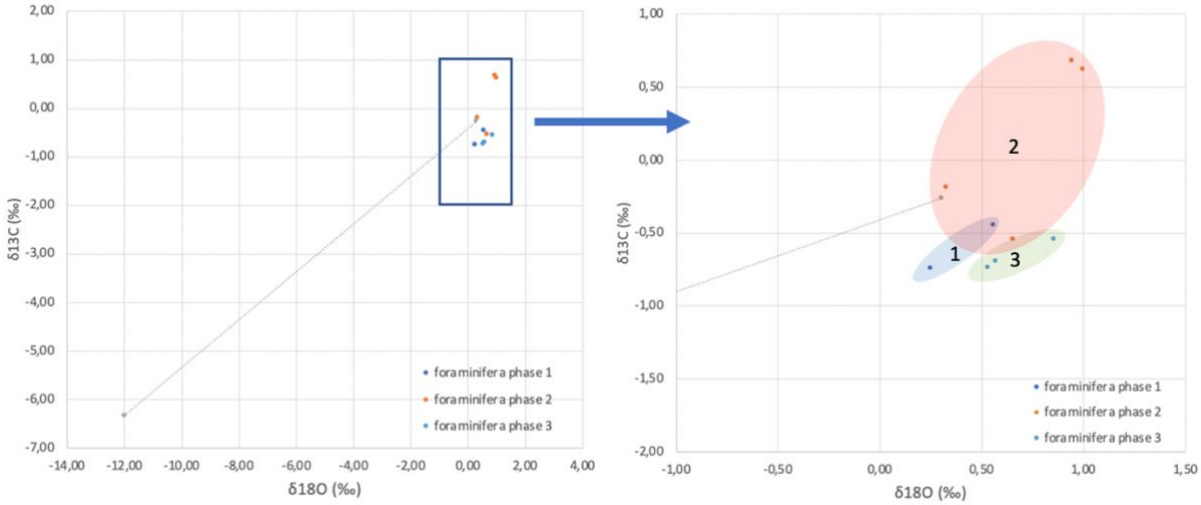

Figure 9: Relation between $\delta^{13}C$ and $\delta^{18}O$ of foraminifera shell carbonates in the Brown Bank Member and the position of the distinguished phases in the mixing line framework.

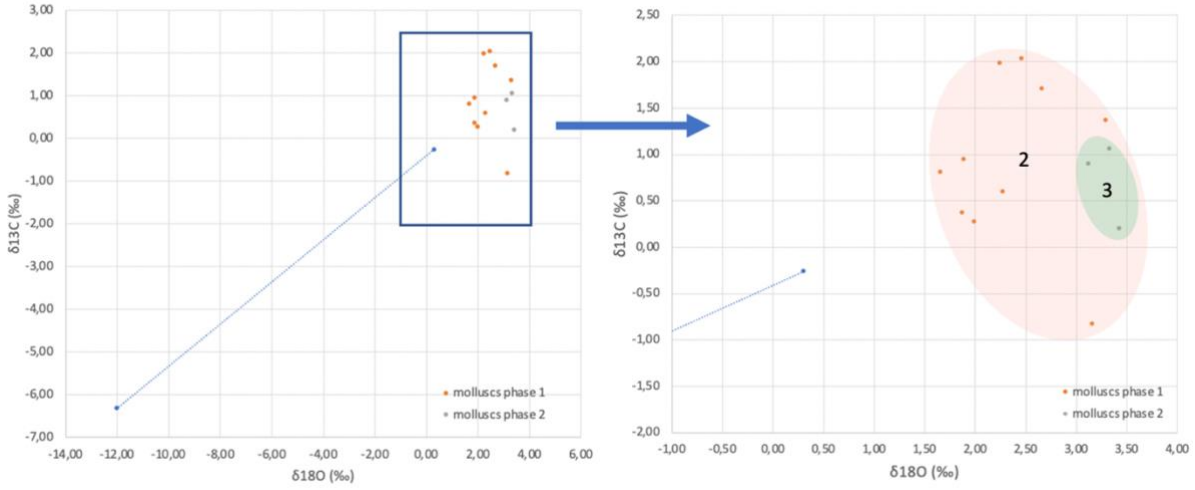

Figure 10: Relation between $\delta^{13}C$ and $\delta^{18}O$ of mollusc shell carbonates in the Brown Bank Member and the position of the distinguished phases in the mixing line framework.

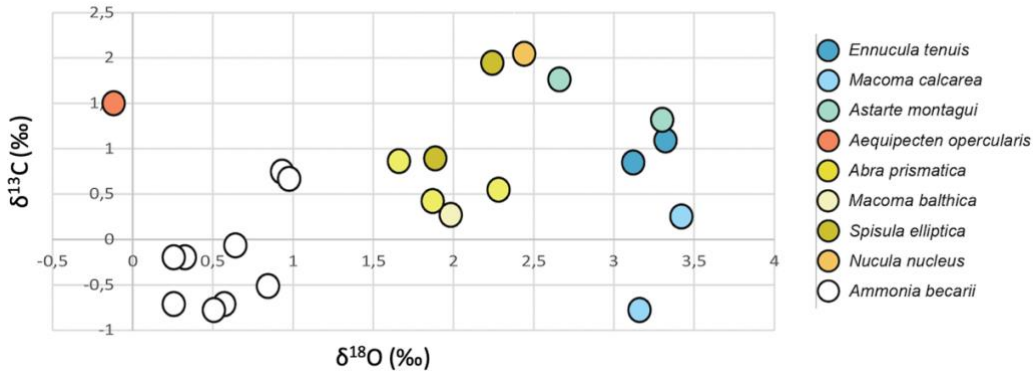

Figure 11: Relation between $\delta^{13}C$ and $\delta^{18}O$ of mollusc and foraminifera shell carbonates in the Brown Bank Member. In general, colder mollusk species show high $\delta^{18}O$ ratios; Aequipecten opercularis likely represents a reworked Eemian (MIS5e) warm-temperate specimen.

5. Discussion

5.1.1 Evolution of the environment at the Amersfoort Basin

The foraminifera isotope data from borehole B32B2417 at Amersfoort show a shift from polyhaline to euhaline conditions and back with an increasing impact of the Rhine River. A synthesis of the environmental evolution is given in figure 12 and will be compared to other records in section *5.1.3*. Salinity and temperature impact on shell carbonate $\delta^{18}O$ content. Eisma et al. (1976) provides a correlation between salinity and $\delta^{18}O$ for Eemian shell carbonates: at a $\delta^{18}O$ value of 0.0‰, a salinity value of ~35‰ will be assumed. Currently, the North Sea mean salinity value varies between 35.2-35.5‰ and the mean temperature varies between 11-12°C (Becker & Pauly, 1996). Due to mixing, salinities will be lower (up to 22‰ in the Western Wadden Sea) near river outlets and estuaries (van Aken, 2008). Assuming change in salinity (S) affected the foraminifera $\delta^{18}O$ content, different trends can be observed per phase. The first phase shows an increasing trend in $\delta^{18}O$ of ~3‰, covering an increase in salinity of approximately 12‰ (~21‰ to ~33‰). This increase in salinity would imply that the water body in the Eemian Amersfoort Basin would have developed from polyhaline brackish water into a euhaline sea with less influence from the river water (fig. 12). Phase 2 shows the highest salinity values between 32‰ and 40‰ (euhaline to metahaline). Phase 3 shows a shift back towards a more brackish environment with a decrease in salinity from ~37‰ to ~26‰. Also, it shows a lowering in relative $\delta^{13}C$ values, indicating an increase in evaporation due to increased residence times. Phase 3 shows a large shift towards phase 4, after which phase 4 shows a decrease in salinity levels from ~37 to ~30‰. This phase overlaps with the mollusc data and shows the presence of *E. ventrosa*, which prefers salinity values of 4-25‰, but they can tolerate lower and higher values (euryhaline conditions; De Bruyne, 2020). Phase 5 shows some lower values and a transition towards a brackish environment again, with an average salinity of ~26‰. This phase shows the largest deviation in the mixing line framework, which is probably due to increased residence times; the $\delta^{13}C$ data show much lower values than the $\delta^{18}O$ data. The $\delta^{13}C$ data imply that the salinity range at phases 1-3 is between 22-28‰ (polyhaline, brackish) and at phase 4 just over 30‰ (euhaline, marine). The $\delta^{13}C$ data show very low salinity levels around 16‰ (mesohaline) at phase 5, indicating low salinity freshwater input.

Reconstructing paleosalinity and paleotemperature yields different values for foraminifera and molluscs. In contrary to the foraminifera data, the mollusc data show a small total salinity change between 3-6‰. This change in salinity is too low. But if temperature affected the isotopic composition of the mollusc shell carbonate, the change in T_W would be about 6-7.5°C. This would be a more assumable change than the foraminifera data indicates. Assuming change in water temperature (T_W) affected the oxygen isotope content in foraminifera, too large fluctuations can be observed. Between phase 1 and 2, the average value for $\delta^{18}O$ increased by 3.47‰, implying a decrease in T_W of approximately 14°C. This seems like a too large number, indicating that the $\delta^{18}O$ content of the foraminifera shells is largely influenced by salinity.

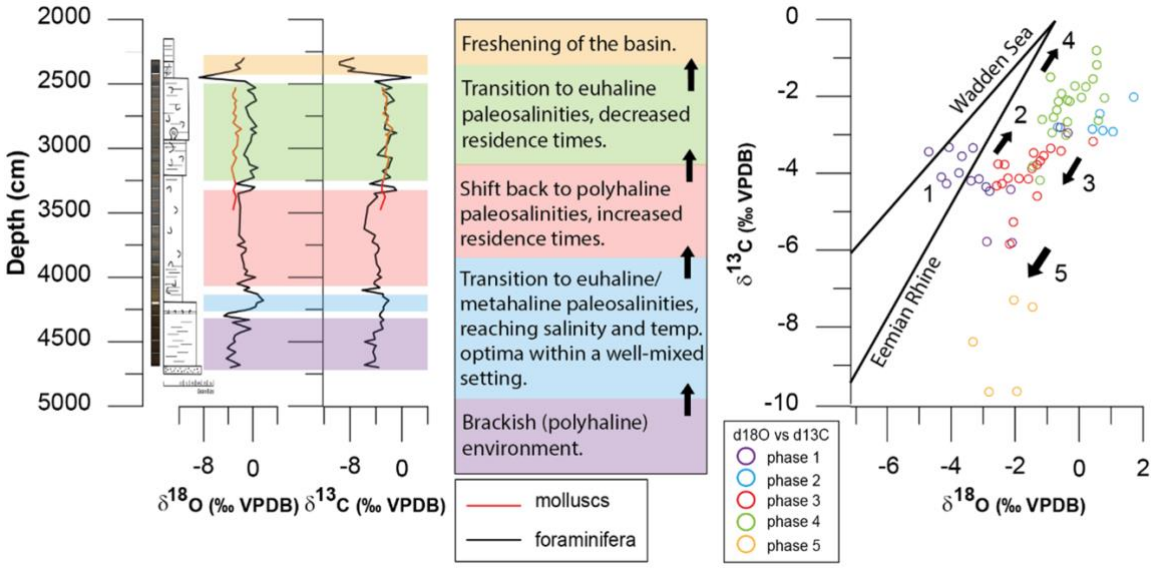

Figure 12: Synthesis of the foraminifera and mollusc data at Amersfoort and their indications for environmental changes. On the right, the relation between $\delta^{18}O$ and $\delta^{13}C$ of the foraminifera data is shown with the Eemian Rhine mixing line and the Wadden Sea mixing line. A shift towards the top right indicates higher marine conditions, while a shift towards the bottom left indicates an increase in influence by fresh river water.

5.1.2 Difference in proxies and implementation of mollusc data

Mollusc and foraminifera isotope ratios show different aspects of the paleoenvironmental evolution. The foraminifera data can be interpreted as a clear overview of salinity change over time but does not account for the temperature change of the water, whilst the mollusc data potentially can. The mollusc data show a smaller variation in isotopic composition (fig. 4; fig. 6). It implies only a small change in salinity, which is almost negligible, but does imply an assumable change in temperature. This could potentially indicate that mollusc shell carbonate growth is more sensitive to temperature than foraminifera shell carbonate growth. To reconstruct paleotemperature from foraminifera would then be more difficult, implying that isotopic composition of mollusc shell carbonate would be a better proxy for reconstructing paleotemperature. Another explanation for this small variation could be that there is only one mollusc species used for the analysis, in contrary to the results of the Brown Bank for which several species were used.

5.1.3 Comparison with other records

The new isotope data add new insights into the evolution of marine ecosystems in the Amersfoort Basin during MIS5e. Cleveringa et al. (2000) investigated a borehole representing the Eemian

succession in the Amersfoort Basin (Amersfoort-1, 2410-1090 cmbs) and showed that the conditions started as a shallow lacustrine environment and changed from a brackish to a more marine environment, reaching depths in the former Amersfoort basin of between -17.80 and -16.80 m NAP. The molluscs present in the top layer and their preservation showed a transition from a tidal marsh to a freshwater environment (Cleveringa et al., 2000). As borehole B32B2417 is located at the depocenter, the sequence is much thicker and more continuous, potentially yielding a more detailed record. Phase 1 of the Amersfoort sequence of B32B2417 implies that low salinities were present in the water body at the Amersfoort Basin. At this period, the water is highly affected by the input of freshwater. However, the results do not indicate a lacustrine environment, but rather a brackish embayment. After that, salinity slowly changes towards higher levels, similar to the environmental changes described by Cleveringa et al. (2000). Also, plant material is present in phase 5, which is also present in the top layer of Cleveringa et al. (2000). Both studies show that mollusc and foraminifera shell carbonate can result in similar interpretations for reconstructing paleosalinity.

When compared to other studies, stable isotope data could also be used to reconstruct time scales. When compared with reconstructed paleotemperatures, timescales can be roughly estimated. Study showed that peak warmth conditions were reached around 128.5-126 kyr BP (Irvali et al., 2012). After that, a cooling event appeared, approximately between 126-124 kyr BP. This cooling event is associated with an isotopic shift in $\delta^{18}O$. For example, the study showed an abrupt decrease of ~0.8‰ in the *N. pachyderma* $\delta^{18}O$ record at ~126 kyr BP occurring over an equivalent to ~120 years (Irvali et al., 2012). This event could match the beginning of phase 1 following the cooling trend towards the end of phase 2. If the match is correct this would imply that phase 1 and 2 would approximately have occurred between ~128.5-124 kyr BP. When compared with reconstructed sea levels, the data show a more detailed timescale record (fig. 13). The reconstructed figure shows a maximum sea level during MIS5e of +6.5 m. Correlation shows that phase 1 and 2 would have occurred between ~130-125.5 kyr BP (Blanchon et al., 2009; Sivan et al., 2016). Reconstructed timescales obtained by the two different comparisons agree but show an error of approximately 1.5 kyr. The second comparison also shows that phase 3 occurred between ~125.5-121.7 kyr BP and phase 4 between ~121.7-117.5 kyr BP (fig. 13). The detailed timescales obtained by correlation with other studies contradict the timescale shown in the introduction section because, according to this study, MIS5e started around 130 kyr BP instead of 128 kyr BP.

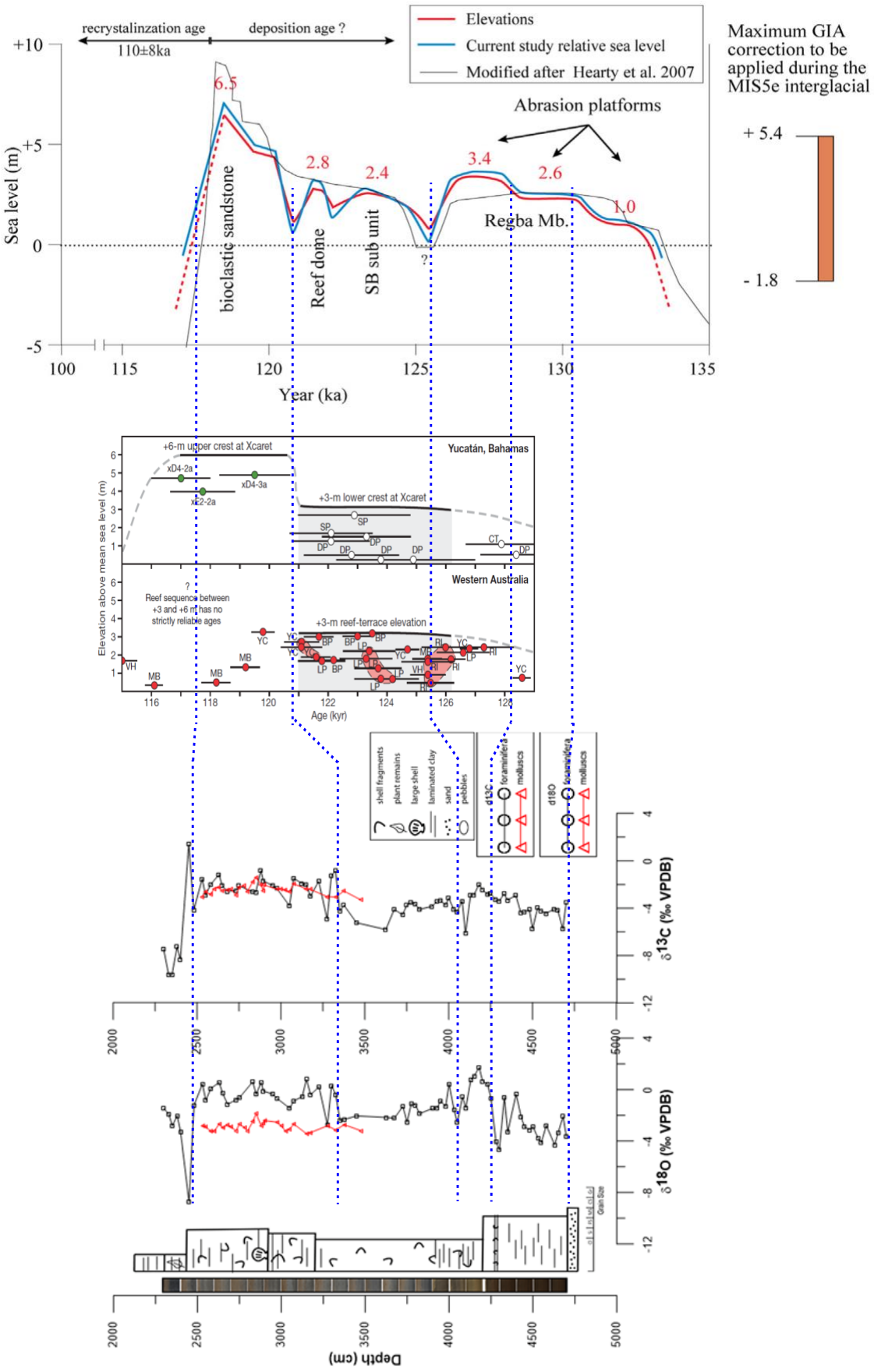

Figure 13: Correlation of the Amersfoort data with reconstructed sea levels during MIS5e (modified from Blanchon et al., 2009, and Sivan et al., 2016).

5.2.1 Evolution of the environment at the Brown Bank Member

Foraminifera isotope ratios in the marine Brown Bank Member show a three-stage temperature evolution. A synthesis of the environmental evolution is given in figure 14 and will be compared to other records in section *5.2.3*. For temperature reconstruction, the relation by Adkins et al. (2002) is used (0.26‰/°C). The foraminifera data show a decrease of ~1.2°C for phase 1. Towards phase 2 the data show a leap of approximately -1.8°C followed by an increasing trend of ~2°C. The third phase shows a decrease of 1.4°C. For salinity reconstruction, the δ^{18}O-S relation by Harwood et al. (2008) and the $\delta^{13}C_{DIC}$-S relation by Wanamaker et al. (2007) are used. The foraminifera data show a small increase of 0.30‰ for δ^{18}O as well as δ^{13}C in the first phase, implying a small increase of ~1‰ (S=~30-36‰). In the second phase, the data than show a leap towards higher salinities (S=~32-38‰), and a decrease in δ^{18}O and δ^{13}C, implying a decrease of approximately 2-3‰. The third phase shows a small increase again of approximately 1‰ in salinity (S=~30-36‰). Salinity levels are higher compared to the Amersfoort Basin, and changes in salinity may be a lot smaller, as the saline water is less influenced by freshwater. This makes temperature a far more important driver for isotope ratio variability.

Mollusc isotope ratios largely agree with the stages but show much stronger temperature regime variability during deposition of the Brown Bank Member with predominant cool to very cold conditions. Phase 2 is very spread out and consist dominantly of species related to moderate temperatures. First it shows an increase of ~2.7°C. The average increase in temperature of the second phase is <1°C, but the total difference in T_W implied by the mollusc data for phase 2 is approximately 6.3°C. Phase 3 shows much lower temperatures; with a leap of approximately -5.5°C. This matches with the arctic species found in phase 3, implying that temperatures may have decreased fundamentally. *Aequipecten opercularis*, a species that prefers warm-temperate climates (fig. 11), is likely a reworked component. The Brown Bank is an Early Weichselian deposit, insinuating that this specimen originated from another climate. It shows much lower values for δ^{18}O than other mollusc species found at the same depth (fig. 11). The position of the molluscan components in the mixing line framework (fig. 9-10) implies highly marine conditions, having almost no influence of river freshwater. Further research is conducted on the Brown Bank Member; a structured paleoecological stable isotope approach could elucidate paleoenvironmental and temperature evolution in greater detail.

Overall, the isotopic composition of the foraminifera and mollusc fauna at the Brown Bank Member from the Early Weichselian show a sharp decrease in temperature with an increase in salinity at first, after which temperatures slowly increased and salinity levels slowly decreased. After that, temperatures and salinity levels decreased, and arctic mollusc species made an appearance. Temperatures were moderate, with a mean salinity level of about 35‰ (all data imply euhaline to metahaline conditions).

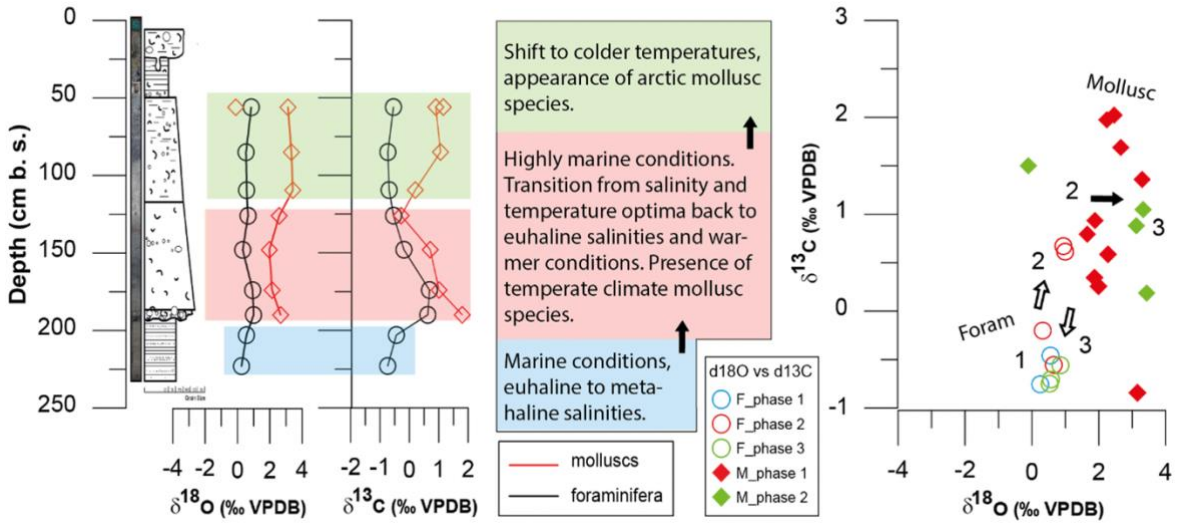

Figure 14: Synthesis of the foraminifera and mollusc data at the Brown Bank Member and their indications for environmental changes. On the right, the relation between $\delta^{18}O$ and $\delta^{13}C$ of the data and shifts within the foraminifera data (arrows with no fill) and the mollusc data (filled arrows) is shown. Note that mixing lines are left out as they are irrelevant because of continuous marine conditions.

5.2.2 Difference in proxies

The proxies show different outcomes and are each more representative as an indicator for temperature- and salinity-related characteristics. The data at Amersfoort alone does not provide enough information to confirm this, but the data at the Brown Bank Member show the same conclusion. The mollusc data show much higher values for changes in salinity and temperature. The lower values retrieved from the foraminifera data seem more likely and representative for change in salinity of the seawater at the Brown Bank Member. Similarly, the higher values retrieved from the mollusc data seem more likely and representative for change in temperature of the seawater at the Brown Bank Member. An explanation for this could be that the growth of shell carbonate in foraminifera shells is highly dependent on salinity levels, whilst the growth of shell carbonate in mollusc shells is highly dependent on temperature levels.

5.2.3 Comparison with other records

Records of other studies show some resemblance in paleotemperature, but there are still differences in interpreting paleosalinity. According to Long et al. (1988), the uppermost Eemian sediments in the southern North Sea are overlain with marine-brackish to freshwater silty clays with silt and fine sand laminae (Brown Bank Formation), deposited in a lagoonal environment during the beginning of the glacial regression. The study mentions that the Brown Bank deposits are extensively bioturbated, explaining the reworked component in the mollusc data. In contrast to their study, the results of this study do not show any determining influence of freshwater nor salinity levels that indicate a brackish environment. Temperature reconstructions of another study by Waaijen et al. (2023) does show similarities (fig. 15). In the study, they made a reconstruction for mean air paleotemperatures for the same borehole (SS22-320-VC14), showing an increasing trend at depths corresponding with phase 2. Air temperature will tend to increase towards the end of phase 3, reaching a mean temperature of 10±2°C but then decreases towards a mean air temperature of 6±2°C. It is also mentioned that the formation was indeed deposited in a marine environment, where the area of the river outlet (that had

subsequent influence on salinity) came closer to the site at the transition from sand to clay (Waaijen et al., 2023). This transition can be seen in the Brown Bank lithology between unit L3 and L4. Within these units, bioturbation was present. Two mollusc samples were taken from unit L4, of which one was the reworked component and the other was an arctic specimen. These samples do not however reveal subsequent information about the salinity, other than relatively high salinity levels. It shows that there is information missing to make valid interpretations of paleosalinity.

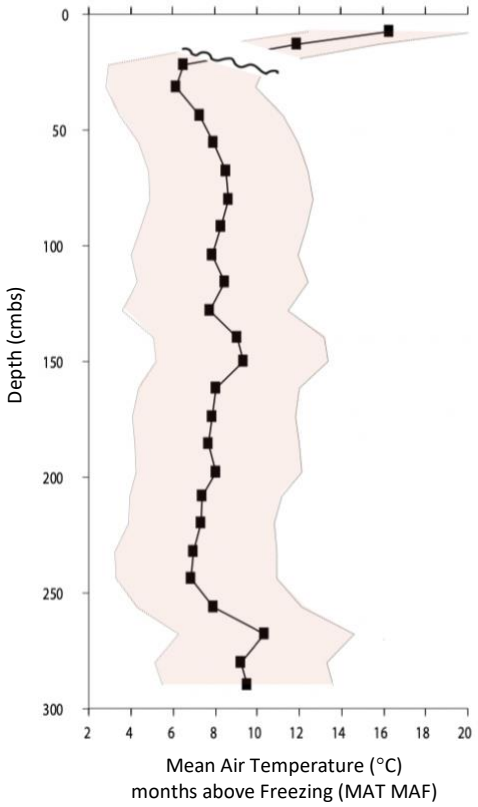

Figure 15: Reconstruction of the paleotemperature at the Brown Bank Member, retrieved from core SS22-320-VC14 (Waaijen et al., 2023).

When compared to the sea level of the last 250,000 years, there are multiple corresponding periods for the depth range of the Brown Bank formation (fig. 16), which is located 22-16 m beneath the water surface (Missiaen et al., 2021). One of the corresponding periods is between ~85-75 ka (fig. 13). This age matches the age of the Brown Bank Member succession of Waaijen et al. (2023) but shows an error of 5 kyr with the described age by Helmens (2014) used in the introduction section.

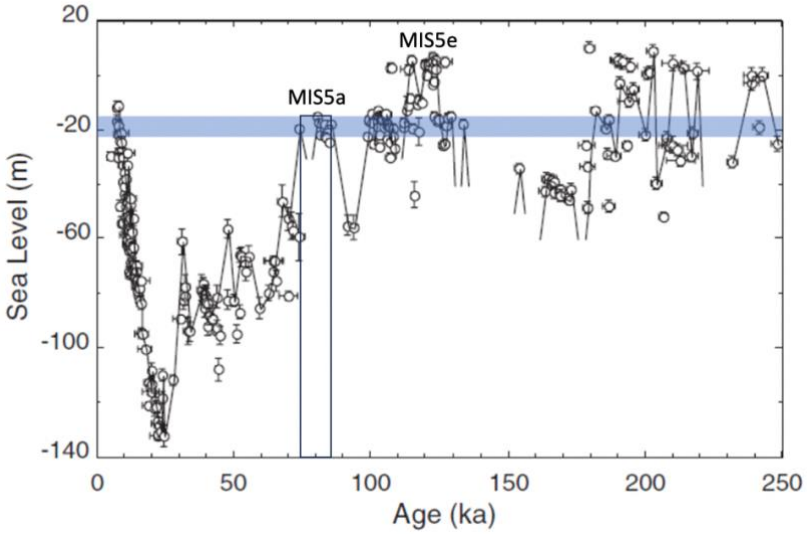

Figure 16: Sea level change over the last 250 kyr. MIS5a is appointed with its corresponding depth and age range. MIS5e is also appointed (modified from Thompson & Goldstein, 2006).

5.3 Recommendations

The usage of different groups as proxies can result in complementary information and to create a clear image with the use of stable isotopes you will need a good approach. To create a clear image, a good overview is important. This can be achieved with chronostratigraphy, where the depth next to a schematic overview of the lithology is given, which is than correlated with a time scale. Furthermore, this study showed that for stable isotope analysis, different species of molluscs are needed to create a more extensive image of changes in paleotemperature. For the benthic foraminifera, the same species can be used for reconstructing paleosalinity. The type of species used may give supplementary information about the environment. Furthermore, different mollusc species can be used because it is easier to recognize an *in situ* component. These components are representative for the conditions of time of deposition of the ambient sediment. At last, the more data is collected, the clearer the image becomes. The absence of mollusc data at the Amersfoort borehole is followed by incomplete interpretation of the local paleotemperature.

6. Conclusions

The use of stable oxygen and carbon isotopes as proxies for reconstructing paleoenvironment and paleoclimate can result in complementary information, and it is relevant to obtain much data for multiple proxies to create a clear image. In the Amersfoort succession, the foraminifera data indicate a shift from polyhaline to euhaline conditions with increasing influence of the Rhine River. The salinity changes inferred from the data suggest the development of a brackish environment into a more marine-like sea. The foraminifera data also suggest increased evaporation due to increased residence time during the final phase. The results show that the isotopic composition in the foraminifera shells of *A. beccarii s.l.* is largely influenced by salinity, in contrast to changes in temperature of ambient water, making them better indicators for paleosalinity for bodies of water that can be largely influenced by river freshwater. The mollusc data, on the other hand, show only a small change in salinity but imply a more significant change in temperature. This suggests that mollusc shell carbonate growth is more sensitive to temperature and therefore have the potential to be better indicators for paleotemperature. When compared with other records, it is noted that foraminifera and mollusc shells

can yield similar interpretations for changes in paleosalinity. However, variations in paleotemperature are more pronounced in mollusc data. In the Brown Bank succession, the foraminifera data indicate a three-stage temperature evolution, while the mollusc data show larger variability in temperature regimes. Different mollusc species are used, yielding larger fluctuations in the mollusc data than the foraminifera data. This makes it easier to interpret the results and supports the idea that mollusc shell carbonate growth is more influenced by temperature changes. The foraminifera data imply smaller changes in salinity in the Brown Bank succession than in the Amersfoort succession, suggesting smaller influence by river freshwater. Compared to other studies, the results show resemblance in changes in paleotemperature but difference in paleosalinity. Also, comparison shows a revised age for MIS5e. The use of multiple proxies is a method to substantiate certain shifts observed in the data, showing the relevance of the usage of multiple proxies for making valid interpretations and therefore reconstructing paleoenvironment and -climate.

Acknowledgements

First, I want to thank Frank Wesselingh (Naturalis) for personally guiding and supporting me through this project, showing me insights of this field of research, and for providing me with samples from the Brown Bank. Second, I want to thank Lucas Lourens (Utrecht University) for his guidance during sample preparation, informative support, and helping me with Grapher and timescale correlation. Furthermore, I want to thank Jeroen Schokker (TNO) for providing me with the necessary information about core B32B2417, Tobias Agterhuis (Utrecht University) for guiding me through the preparation of the samples, and Desmond Eefting (stable isotope laboratory Utrecht University) for helping me with measuring stable isotopes. At last, I want to thank Irene Waaijen (TNO) for providing me with information about the Brown Bank.

References

Adkins, J. F., McIntyre, K., & Schrag, D. P. (2002). The salinity, temperature, and $\delta^{18}O$ of the glacial deep ocean. *Science*, *298*(5599), 1769-1773. DOI:10.1126/science.1076252

Becker, G. A., & Pauly, M. (1996). Sea surface temperature changes in the North Sea and their causes. *ICES Journal of Marine Science*, *53*(6), 887-898. DOI:10.1006/jmsc.1996.0111

Beets, D. J., Meijer, T., Beets, C. J., Cleveringa, P., Laban, C., & Van der Spek, A. J. F. (2005). Evidence for a Middle Pleistocene glaciation of MIS 8 age in the southern North Sea. *Quaternary International*, *133*, 7-19. DOI:10.1016/j.quaint.2004.10.002

Bemis, B. E., Spero, H. J., Bijma, J., & Lea, D. W. (1998). Reevaluation of the oxygen isotopic composition of planktonic foraminifera: Experimental results and revised paleotemperature equations. *Paleoceanography*, *13*(2), 150-160. DOI:10.1029/98PA00070

Blanchon, P., Eisenhauer, A., Fietzke, J., & Liebetrau, V. (2009). Rapid sea-level rise and reef back-stepping at the close of the last interglacial highstand. *Nature*, *458*(7240), 881-884. DOI:10.1038/nature07933

Brewer, S., Guiot, J., Sánchez-Goñi, M. F., & Klotz, S. (2008). The climate in Europe during the Eemian: a multi-method approach using pollen data. *Quaternary Science Reviews*, *27*(25-26), 2303-2315. DOI:10.1016/j.quascirev.2008.08.029

Chen, H., Chen, Y., Li, W., & Li, Z. (2019). Quantifying the contributions of snow/glacier meltwater to river runoff in the Tianshan Mountains, Central Asia. *Global and Planetary Change*, *174*, 47-57. DOI:10.1016/j.gloplacha.2019.01.002

Chenery, C. A., Pashley, V., Lamb, A. L., Sloane, H. J., & Evans, J. A. (2012). The oxygen isotope relationship between the phosphate and structural carbonate fractions of human bioapatite. *Rapid Communications in Mass Spectrometry*, *26*(3), 309-319. DOI:10.1002/rcm.5331

Cleveringa, P., Meijer, T., Van Leeuwen, R. J. W., Wolf, H. D., Pouwer, R., Lissenberg, T., & Burger, A. W. (2000). The Eemian stratotype locality at Amersfoort in the central Netherlands: a re-evaluation of old and new data. *Netherlands Journal of Geosciences/Geologie en Mijnbouw*, *79*(2/3). DOI:10.1017/S0016774600023659

Coplen, T. B. (1988). Normalization of oxygen and hydrogen isotope data. *Chemical Geology: Isotope Geoscience Section*, *72*(4), 293-297. DOI:10.1016/0168-9622(88)90042-5

Dansgaard, W., Johnsen, S.J. Clausen, H. B., Dahl-Jensen, D., Gundestrup, N. S., Hammer, C. U., Steffensen, J. P. (1993). Evidence for general instability of past climate from a 250-kyr ice-core record. *Nature, 364*(6434), 218-220. DOI:10.1038/364218a0

De Bruyne, R. (2020). *Veldgids Schelpen* (2e editie). *KNNV Uitgeverij*.

Eisma, D., Mook, W. G., & Das, H. A. (1976). Shell characteristics, isotopic composition and trace-element contents of some euryhaline molluscs as indicators of salinity. *Palaeogeography, Palaeoclimatology, Palaeoecology*, *19*(1), 39-62. DOI:10.1016/0031-0182(76)90041-9

Epstein, S., Buchsbaum, R., Lowenstam, H. A., & Urey, H. C. (1953). Revised carbonate-water isotopic temperature scale. *Geological Society of America Bulletin*, *64*(11), 1315-1326. DOI:10.1130/0016-7606(1953)64[1315:RCITS]2.0.CO;2

Finné, M., Salonen, S., Frank, N., Helmens, K. F., Schröder-Ritzrau, A., Deininger, M., & Holzkämper, S. (2019). Last Interglacial Climate in Northern Sweden—Insights from a Speleothem Record. *Quaternary*, *2*(3), 29. DOI:10.3390/quat2030029

Gareis, J. A., & Lesack, L. F. (2020). Ice-out and freshet fluxes of CO_2 and CH_4 across the air–water interface of the channel network of a great Arctic delta, the Mackenzie. *Polar Research*. DOI:10.33265/polar.v39.3528

Ge, T., Luo, C., Ren, P., Zhang, H., Fan, D., Chen, H., ... & Wang, X. (2022). Stable carbon isotopes of dissolved inorganic carbon in the western North Pacific Ocean: Proxy for water mixing and dynamics. *Frontiers in Marine Science*, 1903. DOI:10.3389/fmars.2022.998437

Gebbie, G., Peterson, C. D., Lisiecki, L. E., & Spero, H. J. (2015). Global-mean marine $\delta^{13}C$ and its uncertainty in a glacial state estimate. *Quaternary Science Reviews*, *125*, 144-159. DOI:10.1016/j.quascirev.2015.08.010

Gurney, S. D., & Lawrence, D. S. L. (2004). Seasonal trends in the stable isotopic composition of snow and meltwater runoff in a subarctic catchment at Okstindan, Norway. *Hydrology Research*, *35*(2), 119-137. DOI:10.2166/nh.2004.0009

Harting, P. (1874). De bodem van het Eemdal. Verslagen en Mededelingen van de Koninklijke Akademie van Wetenschappen, afdeling Natuurkunde II 8: 282-290.

Harwood, A. J., Dennis, P. F., Marca, A. D., Pilling, G. M., & Millner, R. S. (2008). The oxygen isotope composition of water masses within the North Sea. *Estuarine, Coastal and Shelf Science*, *78*(2), 353-359. DOI:10.1016/j.ecss.2007.12.010

Hayward, B. W., Holzmann, M., & Tsuchiya, M. (2019). Combined molecular and morphological taxonomy of the beccarii/T3 group of the foraminiferal genus Ammonia. *Journal of Foraminiferal Research*, *49*(4), 367-389. DOI:10.2113/gsjfr.49.4.367

Hayward, B. W., Holzmann, M., Pawlowski, J., Parker, J. H., Kaushik, T., Toyofuku, M. S., & Tsuchiya, M. (2021). Molecular and morphological taxonomy of living Ammonia and related taxa (Foraminifera) and their biogeography. *Micropaleontology*, *67*(2-3), 109-274. DOI:10.47894/mpal.67.2-3.01

Helmens, K. F. (2014). The Last Interglacial–Glacial cycle (MIS 5–2) re-examined based on long proxy records from central and northern Europe. *Quaternary Science Reviews*, *86*, 115-143. DOI:10.1016/j.quascirev.2013.12.012

IPCC, 2021. Climate Change 2021: the Physical Science Basis. Contribution of Working Group I to the Sixth Assessment Report of the Intergovernmental Panel on Climate Change. Cambridge University Press (in press).

Irvalı, N., Ninnemann, U. S., Galaasen, E. V., Rosenthal, Y., Kroon, D., Oppo, D. W., ... & Kissel, C. (2012). Rapid switches in subpolar North Atlantic hydrography and climate during the Last Interglacial (MIS 5e). *Paleoceanography*, *27*(2). DOI:10.1029/2011PA002244

Kasse, C., Van Der Woude, J. D., Woolderink, H. A., & Schokker, J. (2022). Eemian to Early Weichselian regional and local vegetation development and sedimentary and geomorphological controls, Amersfoort Basin, The Netherlands. *Netherlands Journal of Geosciences*, *101*. DOI:10.1017/njg.2022.4

Katrantsiotis, C., Norström, E., Smittenberg, R. H., Salonen, J. S., Plikk, A., & Helmens, K. (2021). Seasonal variability in temperature trends and atmospheric circulation systems during the Eemian (Last Interglacial) based on n-alkanes hydrogen isotopes from Northern Finland. *Quaternary Science Reviews*, *273*, 107250. DOI:10.1016/j.quascirev.2021.107250

Kendall, C., & Caldwell, E. A. (1998). Fundamentals of isotope geochemistry. In *Isotope tracers in catchment hydrology* (pp. 51-86). Elsevier. DOI:10.1016/B978-0-444-81546-0.50009-4

Law, M. (2013). Bryozoans in archaeology. *Internet Archaeology*, (35). DOI:10.11141/ia.35.3

Long, D., Laban, C., Streif, H., Cameron, T. D. J., & Schüttenhelm, R. T. E. (1988). The sedimentary record of climatic variation in the southern North Sea. *Philosophical Transactions of the Royal Society of London. B, Biological Sciences*, *318*(1191), 523-537. DOI:10.1098/rstb.1988.0022

Milano, S., Pop, E., Kuijper, W., Roebroeks, W., Gaudzinski-Windheuser, S., Penkman, K., ... & Britton, K. (2020). Environmental conditions at the Last Interglacial (Eemian) site Neumark-Nord 2, Germany inferred from stable isotope analysis of freshwater mollusc opercula. *Boreas*, *49*(3), 477-487. DOI:10.1111/bor.12437

Missiaen, T., Fitch, S., Harding, R., Muru, M., Fraser, A., De Clercq, M., ... & Gaffney, V. (2021). Targeting the Mesolithic: interdisciplinary approaches to archaeological prospection in the Brown Bank area, southern North Sea. *Quaternary International*, *584*, 141-151. DOI:10.1016/j.quaint.2020.05.004

Mook, W. G. (1970). Stable carbon and oxygen isotopes of natural water in the Netherlands. *Isotope hydrology, 1970*, 163-190.

NASA Earth Observatory. (2005). *Paleoclimatology: The Oxygen Balance*. https://earthobservatory.nasa.gov/features/Paleoclimatology_OxygenBalance

O'Neil, J. R., Clayton, R. N., & Mayeda, T. K. (1969). Oxygen isotope fractionation in divalent metal carbonates. *The Journal of Chemical Physics*, *51*(12), 5547-5558. DOI:10.1063/1.1671982

Por, F. D. (1972). "Hydrobiological notes on the high-salinity waters of the Sinai Peninsula". *Marine Biology*. **14** (2): 111–119. DOI:10.1007/BF00373210

Schrag, D. P., Adkins, J. F., McIntyre, K., Alexander, J. L., Hodell, D. A., Charles, C. D., & McManus, J. F. (2002). The oxygen isotopic composition of seawater during the Last Glacial Maximum. *Quaternary Science Reviews*, *21*(1-3), 331-342. DOI:10.1016/S0277-3791(01)00110-X

Schultz, E. T., & McCormick, S. D. (2012). Euryhalinity in an evolutionary context. *Fish physiology*, *32*, 477-533. DOI:10.1016/B978-0-12-396951-4.00010-4

Shimamura, M., Oba, T., Xu, G., Lu, B., Wang, L., Murayama, M., ... & Winter, A. (2005). Fidelity of δ18O as a proxy for sea surface temperature: Influence of variable coral growth rates on the coral Porites lutea from Hainan Island, China. *Geochemistry, Geophysics, Geosystems*, *6*(9). DOI:10.1029/2005GC000966

Sivan, D., Sisma-Ventura, G., Greenbaum, N., Bialik, O. M., Williams, F. H., Tamisiea, M. E., ... & Stein, M. (2016). Eastern Mediterranean sea levels through the last interglacial from a coastal-marine

sequence in northern Israel. *Quaternary Science Reviews*, *145*, 204-225. DOI:10.1016/j.quascirev.2016.06.001

Thompson, W. G., & Goldstein, S. L. (2006). A radiometric calibration of the SPECMAP timescale. *Quaternary Science Reviews*, *25*(23-24), 3207-3215. DOI:10.1016/j.quascirev.2006.02.007

Turney, C. S., Jones, R. T., McKay, N. P., Van Sebille, E., Thomas, Z. A., Hillenbrand, C. D., & Fogwill, C. J. (2020). A global mean sea surface temperature dataset for the Last Interglacial (129–116 ka) and contribution of thermal expansion to sea level change. *Earth System Science Data*, *12*(4), 3341-3356. DOI:10.5194/essd-12-3341-2020

van Aken, H. M. (2008). Variability of the salinity in the western Wadden Sea on tidal to centennial time scales. *Journal of Sea Research*, *59*(3), 121-132. DOI:10.1016/j.seares.2007.11.001

van Aken, H. M. (2008). Variability of the water temperature in the western Wadden Sea on tidal to centennial time scales. *Journal of Sea Research*, *60*(4), 227-234. DOI:10.1016/j.seares.2008.09.001

van Leeuwen, R. J., Beets, D. J., Aleid Bosch, J. H., Burger, A. W., Cleveringa, P., Harten, D. V., ... & Wolf, H. D. (2000). Stratigraphy and integrated facies analysis of the Saalian and Eemian sediments in the Amsterdam-Terminal borehole, the Netherlands. *Netherlands Journal of Geosciences/Geologie en Mijnbouw*, *79*(2/3). DOI:10.1017/S0016774600023647

Versteegh, E. A., Troelstra, S. R., Vonhof, H. B., & Kroon, D. (2009). Oxygen isotope composition of bivalve seasonal growth increments and ambient water in the rivers Rhine and Meuse. *Palaios*, *24*(8), 497-504. DOI:10.2110/palo.2008.p08-071r

Versteegh, E. A., Vonhof, H. B., Troelstra, S. R., Kaandorp, R. J., & Kroon, D. (2010). Seasonally resolved growth of freshwater bivalves determined by oxygen and carbon isotope shell chemistry. *Geochemistry, Geophysics, Geosystems*, *11*(8). DOI:10.1029/2009GC002961

Waaijen, I., Busschers, F., Donders, T., Schokker, J., van Heteren, S., Peterse, F., Martinez-Sosa, P. (2023). Long-distance correlation of Early Weichselian (MIS5d-a) deposits across the southern North Sea region. *TNO Geological Survey of the Netherlands.*

Wanamaker Jr, A. D., Kreutz, K. J., Borns Jr, H. W., Introne, D. S., Feindel, S., Funder, S., ... & Barber, B. J. (2007). Experimental determination of salinity, temperature, growth, and metabolic effects on shell isotope chemistry of Mytilus edulis collected from Maine and Greenland. *Paleoceanography*, *22*(2). DOI:10.1029/2006PA001352

Wesselingh, F. P., Meijer, T., Harting, R., Bakker, M., & Busschers, F. S. (2023). New marine warm-temperate molluscan assemblage demonstrates warm conditions during the Middle Pleistocene of the North Sea Basin. *Netherlands Journal of Geosciences*, *102*, e3. DOI:10.1017/njg.2023.1

Yan, H., Dettman, D. L., Chen, J., & Shen, N. (2020). $\delta^{13}C$ in Corbicula fluminea shells: Implication for dissolved inorganic carbon reconstruction. *Geochemical Journal*, *54*(2), 71-79. DOI:10.2343/geochemj.2.0585

Appendix 1: Descriptions of the Amersfoort core and Brown Bank Member core, per section

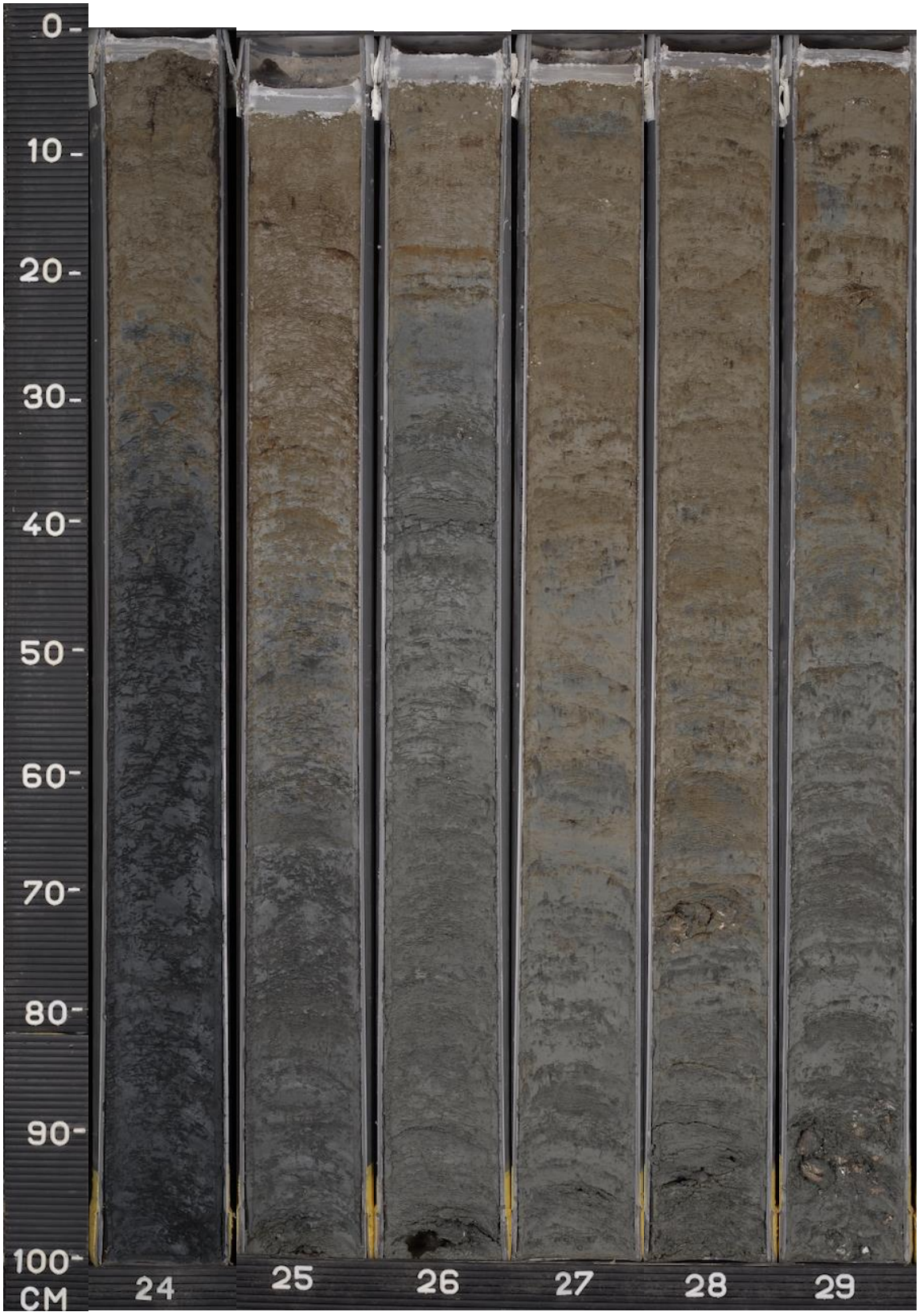

Core photographs of borehole B32B2417 (Amersfoort): interval of 2304-2900 cmbs. Photo courtesy of TNO geological survey of the Netherlands.

Section 24
Comprises a depth of 2303-2400cm. Shows dark brown color on top, and gradually changes to dark grey around 2330cm depth. Remains grey to the bottom.

Section 25
Comprises a depth of 2406-2500cm. Shows dark brown color on top, and gradually changes to grey around 2440cm depth. Remains grey to the bottom. Shows some light grey bands between 2420 and 2443cm.

Section 26
Comprises a depth of 2503-2600cm. Shows dark brown color on top and shows a fast change to grey around 2520cm depth. Remains grey to the bottom. It contains a reddish band around 2518cm and some shell fragments around 2533cm.

Section 27
Comprises a depth of 2603-2700cm. Shows dark brown color on top and shows a slow gradual change to grey around 2640cm depth. Remains grey to the bottom. Contains some shell fragments around 2615 and 2627cm.

Section 28
Comprises a depth of 2702-2800cm. Shows dark brown color on top and shows a slow gradual change to grey between 2740-2780cm depth. Remains grey to the bottom. Contains shell fragments around 2773cm.

Section 29
Comprises a depth of 2802-2900cm. Shows dark brown color on top and shows a slow gradual change to grey between 2810-2850cm depth. Remains grey to the bottom. Contains shell band between 2886-2900cm, containing a *venerupis* species.

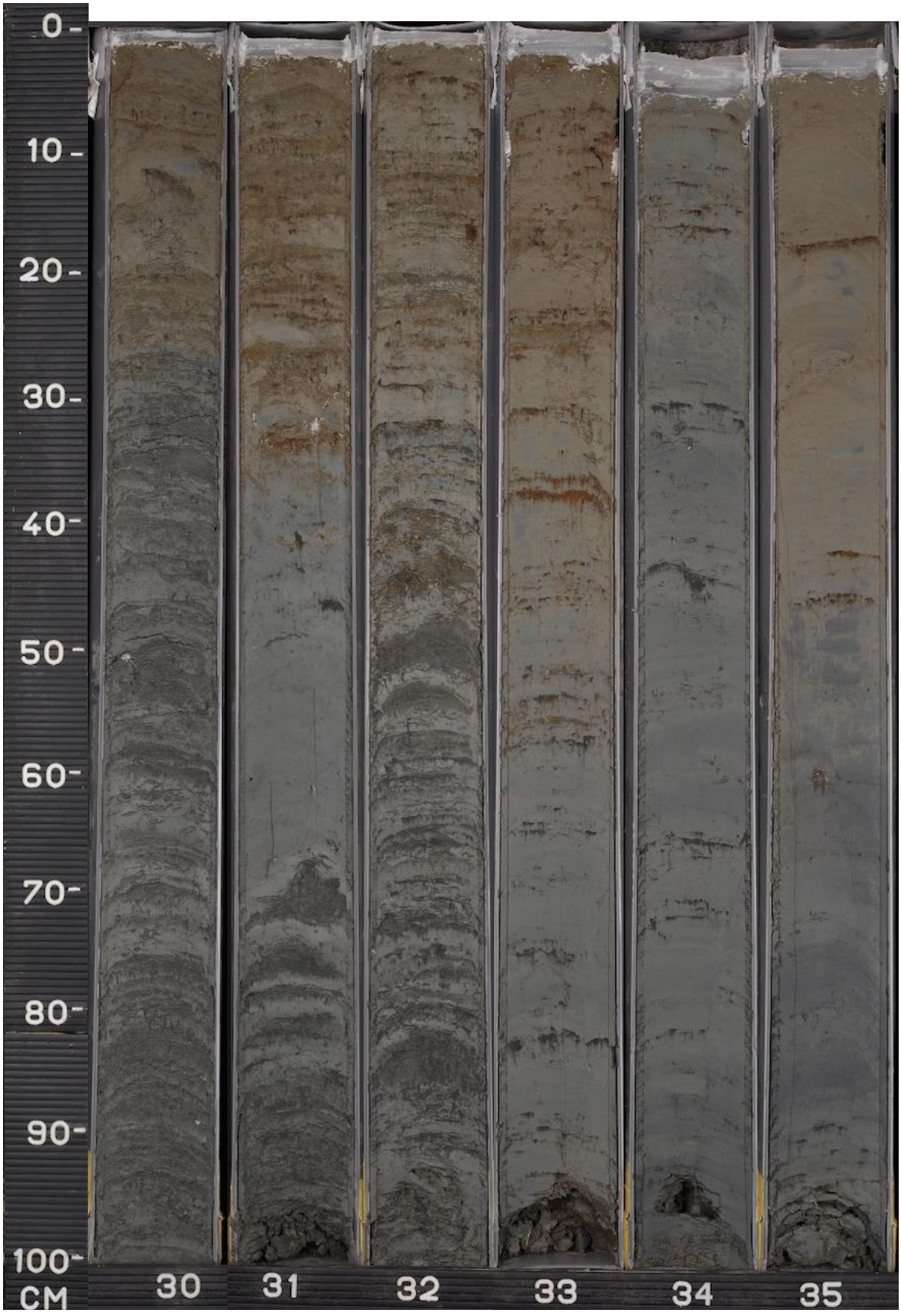

Core photographs of borehole B32B2417 (Amersfoort): interval of 2901-3500 cmbs. Photo courtesy of TNO geological survey of the Netherlands.

Section 30
Comprises a depth of 2901-3000cm. Shows dark brown color on top, and gradually changes to grey around 2925cm depth. Remains grey to the bottom. Shows layering with lighter colors in the grey part. Contains a shell fragment at 2950cm.

Section 31
Comprises a depth of 3001-3100cm. Shows dark brown color at the top, and changes to grey around 3035cm. Remains grey to the bottom. Shows layering in the brown part and layering in the grey part between 3070-3100cm. Contains shell fragments and a reddish band around 3010cm.

Section 32
Comprises a depth of 3101-3200cm. Dark brown at the top, which gradually changes to grey up to 3130cm. Shows layering throughout the section and contains a dark brown colored band between 3140-3146cm.

Section 33
Comprises a depth of 3205-3300cm. Dark brown at the top, which gradually changes to grey up to 3130cm. Shows dark colored bands throughout the section at 3235cm (reddish), 3231cm (reddish), 3238cm (reddish), and layering between 3252-3259cm.

Section 34
Comprises a depth of 3305-3400cm. Grey with a brownish hue at the top, which changes to grey at 3315cm. Shows some dark grey bands at 3315, 3331, 3345, and 3367cm. No further layering.

Section 35
Comprises a depth of 3401-3500cm. Dark brown at the top, which gradually changes to grey up to 3450cm. Shows a clean section without layering but contains some dark colored bands at 3418cm (reddish) and 3448cm (greyish/reddish).

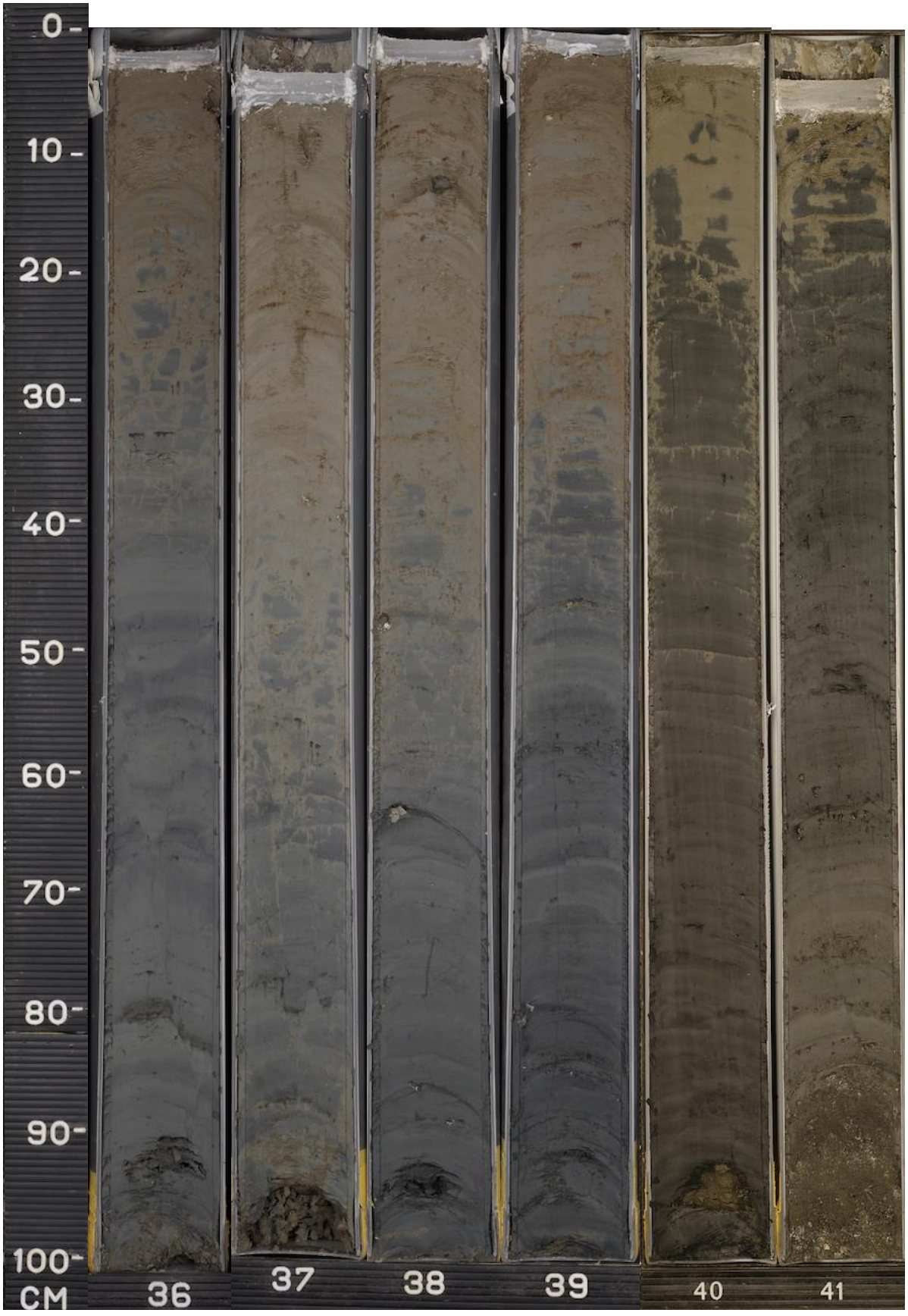

Core photographs of borehole B32B2417 (Amersfoort): interval of 3503-4100 cmbs. Photo courtesy of TNO geological survey of the Netherlands.

Section 36
Comprises a depth of 3503-3600cm. Dark brown at the top, which gradually changes to grey up to 3540cm. Shows a clean section without layering but contains some dark colored bands between 3547-3567cm (dark grey) and at 3581cm (dark grey).

Section 37
Comprises a depth of 3605-3700cm. Dark brown at the top, which gradually changes to grey up to 3660cm. Shows a clean section without layering but contains some dark colored bands at 3678cm and 3687cm.

Section 38
Comprises a depth of 3701-3800cm. Dark brown at the top, which gradually changes to grey up to 3760cm. Shows a clean section without layering but contains darker grey colored bands at 3749 and 3764. Also contains shell fragments at 3749 and 3764cm.

Section 39
Comprises a depth of 3801-3900cm. Dark brown at the top, which gradually changes to grey up to 3840cm. Shows a clean section without layering but contains darker grey colored bands throughout the grey colored area. Shell fragment at 3847cm.

Section 40
Comprises a depth of 3901-4000cm. Yellowish-brown at the top, which gradually changes to dark brown between 3910-3940cm. Shows layering throughout the section and contains some darker colored bands at 3975 and 3980cm.

Section 41
Comprises a depth of 4001-4100cm. Yellowish-brown at the top, which gradually changes to dark brown between 4010-4020cm. Changes to a dark yellowish-brown color at 4085cm and remains that color to the bottom. This part also contains shell fragments. Shows layering throughout the section. Contains a darker colored band at 4053cm, some dark speckles at 4063cm, and a dark yellowish band at 4077cm.

Core photographs of borehole B32B2417 (Amersfoort): interval of 4101-4700 cmbs. Photo courtesy of TNO geological survey of the Netherlands.

Section 42
Comprises a depth of 4101-4200cm. Shows a light brown color throughout the section, which is layered and contains bands over the whole section. Contains shell fragments at 4105, 4111, 4128, 4172, and 4187cm.

Section 43
Comprises a depth of 4216-4300cm. Shows a brown color that gradually changes to a darker brown color throughout the section, which is layered and contains bands over the whole section. It has a shell fragment band around 4222cm and contains small shell fragments throughout the whole section.

Section 44
Comprises a depth of 4301-4400cm. Shows a dark brown color throughout the section, which is layered and contains bands over the whole section. Also contains small shell fragments throughout the whole section.

Section 45
Comprises a depth of 4401-4500cm. Shows a dark brown color throughout the section, which is layered and contains bands over the whole section. Also contains small shell fragments throughout the whole section and a larger shell fragment around 4421cm. Shows a very dark brown band at 4475cm.

Section 46
Comprises a depth of 4501-4600cm. Shows a dark brown color throughout the section, which is layered and contains bands over the whole section. Also contains small shell fragments throughout the whole section.

Section 47
Comprises a depth of 4601-4700cm. Shows a dark brown color throughout the section, which is layered and contains bands over the whole section. At the first 10cm and last 10cm of the section, the brown color is darker than the other parts of the section. Also contains small shell fragments throughout the whole section.

Description of the Brown Bank Member, per section, section 1-3

Core photographs of borehole SS22-320-VC14 (Brown Bank Member): interval of 8-233 cmbs. Photo courtesy of TNO geological survey of the Netherlands.

Section 1/3
This section is the top section and starts at a depth of 8cm because of a hiatus at the top. The bottom of the section is located at 35cm. The sediment consists of brownish-grey blackish sand and clay and contains shell fragments throughout the section. It shows 3 large rounded pebbles at 3-5cm and 18-20cm and an elongated rounded pebble at 23cm. The bottom of the section consists of dark stiff clay.

Section 2/3
This section is located at 35-135cm and has a dark grey color. At the top it has some material from the sand from the layer above, indicating bioturbation. It has a total depth of 1m. At 18cm (as seen from the scale on the left), there is a layer with some sandy material. Further down, it shows some layering. Between 20-45cm, there are some bodies of heavier grained sediment with some shell fragments. From 50-100cm, the dark clay becomes lighter of color.

Section 3/3
This section is located at a depth of 135-233cm and has a total depth of 98cm. It shows some light grey spots at the top and becomes more brownish downward throughout the whole section and laminae become more visible. At a depth of 52-60cm, a big shell of about 4cm it present, which is contained in a layer of black-greyish sand. At that depth, there are also a lot of shell fragments visible. The bottom of the section consists out of stiff clay.

Appendix 2: Lithology of the Brown Bank Member (obtained via TNO Geological survey of the Netherlands)

Project	Brown Bank	**Borehole - VIBRO**	SS22_320_VC14
Lat	52.70599388	**Long**	3.35766505
Elevation	EMODNET msl: -44.21m PES: -44.80m	**Date drilled**	12/06/2022
Date to laboratory		**Date recorded**	14/02/2023 – Morgan Vervoort, Kimberly Demeestere, Ruth Plets
Date sampled		**Location core**	VLIZ

Depth below ground surface (m)	**Depth O.D.**	**Lithological description**	**Type of contact + notes**
0-0.25		Brownish grey very fine sand and clay with shell fragments throughout. @0.18-0.2m: 3 large rounded pebbles of 3-5cm @0.23m: 1 elongated rounded pebble	
		--- ---	Gradual
0.25-0.52		Dark grey bioturbated stiff clay (with bioturbation filled with material from above) @0.32-0.33m: black organic rich lens @0.505-0.535m: lens of fine sand @0.52m: granules on boundary	* 0.49m: pollen sample TNO
		--- ---	Granules on gradual boundary
0.52-1.19		Fining upwards from fine sand to clayey silt, grey to dark grey. Patches of shell fragments and granules/small pebbles throughout	* 0.84m: pollen sample TNO * 1.14m: pollen sample TNO
		--- ---	gradual
1.19 – 1.89		Fining upwards from medium-coarse sand to fine sand, grey. Shell fragments throughout @1.45-1.48m and 1.51-1.52m: granules-medium pebbles @1.86-1.89m: big shell (4-5cm) – does this belong to this layer or layer below?	* 1.51m: pollen sample TNO
		--- ---	clear
1.89-1.93		Black-grey medium sand with shell fragments and medium pebbles	
		--- ---	Clear
1.93-2.33		Brown-green silt-clay and fine sand lamina with mica's throughout @2.21-2.22m: grey thick lamina	* 2.04m: pollen sample TNO * 2.23m: pollen sample TNO
		--- ---	
2.33	END CORE		